METEOROLOGISKA INSTITUTIONEN
vid
KUNGL. UNIVERSITETET
UPPSALA

LEIF ENGER

NUMERICAL BOUNDARY LAYER MODELING WITH APPLICATION TO DIFFUSION

PART II

A HIGHER ORDER CLOSURE DISPERSION MODEL

REPORT NO. 71

UPPSALA 1983

LEIF ENGER

NUMERICAL BOUNDARY LAYER MODELING WITH APPLICATION TO DIFFUSION

PART II

A HIGHER ORDER CLOSURE DISPERSION MODEL

REPORT NO. 71

UPPSALA 1983

UNIV.
LEIDEN
BIBL.

Doctoral Thesis at the University of Uppsala 1983

ABSTRACT

Enger, L., 1983. Numerical boundary layer modeling with application to diffusion. Part II. A higher order closure dispersion model. *Department of Meteorology, University of Uppsala. Report No 71.* 45 pp. ISBN 91-506-0386-8.

A two-dimensional higher order closure dispersion model has been developed. A Gaussian assumption is applied for the cross-wind distribution, enabling us to solve the dispersion from a point source with a two-dimensional numerical model. Our model uses mean wind and turbulence quantities from the two-dimensional second order atmospheric boundary layer model presented in Part I. The cross-wind standard deviation is derived from Eulerian velocity spectra with the assumption that $\beta = 4.0$. Simulations with the model are compared with Willis' and Deardorff's laboratory experiments (Deardorff and Willis (1975), Willis and Deardorff (1978 and 1981)) and with results obtained with the Lagrangian model of Lamb (1982) for the convective boundary layer. The results show that the model quite well simulates the dispersion from a point source in a convective layer.

A simulation of dispersion has also been carried out in a case with horizontally heterogeneous conditions. It represents an island fumigation of the plume from an elevated point source situated on an upwind coast line, the stratification over the water in between the source and the island being stable. The result of the simulation appears reasonable.

A verification has also been performed against data from a tracer experiment with horizontally heterogeneous conditions during near neutral stratification. The result of the simulation is in very good agreement with the experimental data.

L. Enger, Department of Meteorology, University of Uppsala, Box 516, S-751 20 Uppsala, Sweden.

ISBN 91-506-0386-8

© Leif Enger
Printed in Sweden by
Department of Meteorology
Uppsala University, 1983

Digitized by the Internet Archive
in 2026

https://archive.org/details/IA41549218_0011

C O N T E N T S

		page
	ABSTRACT	2
1	INTRODUCTION	4
2	DESCRIPTION OF THE MODEL	5
2.1	*Governing equations*	5
2.2	*The model coefficients*	7
2.3	*The gridsystem and the finite difference scheme*	9
2.4	*Initial and boundary conditions*	10
2.5	*Determination of the standard deviations*	12
3	RESULTS	20
	SUMMARY AND CONCLUSIONS	27
	ACKNOWLEDGEMENTS	28
	REFERENCES	29
	FIGURES	31

INTRODUCTION

As evidenced by Pasquill's book (1974) air pollution modelling has proceeded along several principally different lines. In the USA and the western European countries the main emphasis has been put on the Gaussian approach. In the USSR, however, most work has emerged from solutions of the so called semi-emperical diffusion equation (see e.g. Berlyand, 1971). Both these approaches have their distinct weak points, as clearly shown by Pasquill (1974). The appearence of higher-order closure models opens up new avenues of research for the atmosphere boundary layer flow. The main advantages with this approach compared to older models can be summarized accordingly. The higher order closure parametrization removes some of the principal weaknesses of the K-assumption inherent in the semi-empirical diffusion equation approach as well as, of course, the rather ad hoc assumptions underlying the Gaussian approach.At the same time it enables explicit treatment of horizontal inhomogeniety and unsteadiness.

The main difficulty inherent in all higher-order closure work is the parametrization of the higher-order terms and the proper determination of the resulting numerical parameters. This can only be done by comparison with measurements. Fortunately numerous data are now available on the structure of the boundary layer itself, in particular for the daytime convective layer (e.g. Clarke, 1971 and Kaimal et al, 1976). But now fundamental data are also available on dispersion from a point source through a deep convective layer (e.g. Deardorff and Willis, 1975 and Lamb, 1978).

In the present paper a two-dimensional diffusion model is presented which uses mean wind and turbulence quantities from a second order closure model developed by the author (Enger, 1983). The model is tested against results from surface layer measurements (Högström, 1964 and Nieustadt, 1980), water-tank experiments (Willis and Deardorff, 1978, Deardorff and Willis, 1975 and Willis and Deardorff, 1981) and also with another type of diffusion model (Lamb, 1982). Furthermore the model has been tested against a tracer experiment carried out in a near neutral boundary layer.

2 DESCRIPTION OF THE MODEL

The model in this report deals with dispersion from a point source. The dispersion is studied by using a two-dimensional numerical model. Dispersion from a point source is of course a three-dimensional problem. To be able to use a two-dimensional numerical model we will solve the lateral dispersion with the aid of a Gaussian assumption for the cross-wind distribution and calculated standard deviation for the plume.

The dispersion of a gas from a point source in the atmosphere depends on the mean wind and turbulence field. To get the wind, turbulence and temperature field we have used a two-dimensional wind model (Enger, 1983).

The present model is an Euleran diffusion model, that is it starts from the mass continuity equation, $\frac{\partial C}{\partial t} + U\frac{\partial C}{\partial x} + V\frac{\partial C}{\partial y} + W\frac{\partial C}{\partial z} = -\frac{\partial \overline{uc}}{\partial x} - \frac{\partial \overline{vc}}{\partial y} - \frac{\partial \overline{wc}}{\partial z}$. A Lagrangian model is instead working with probability density functions, see Lamb, 1978 for example.

2.1 *Governing equations*

We start with the diffusion equation

$$\frac{\partial C}{\partial t} + U\frac{\partial C}{\partial x} + V\frac{\partial C}{\partial y} + W\frac{\partial C}{\partial z} = -\frac{\partial}{\partial x}(\overline{uc}) - \frac{\partial}{\partial y}(\overline{vc}) - \frac{\partial}{\partial z}(\overline{wc}) \qquad (1a)$$

where
C is the concentration,
U, V and W are the mean wind in x-, y- and z-direction respectively and
$\overline{uc}$, $\overline{vc}$ and $\overline{wc}$ are the turbulent fluxes in the different directions.

Now let us also set the x-axis in the mean wind direction at the source height. The streamwise diffusion $\frac{\partial}{\partial x}(\overline{uc})$ in our applications is much less than the advection term $U\frac{\partial C}{\partial x}$ which means that the diffusion equation (1a) is reduced to

$$\frac{\partial C}{\partial t} + U\frac{\partial C}{\partial x} + V\frac{\partial C}{\partial y} + W\frac{\partial C}{\partial z} = -\frac{\partial}{\partial y}(\overline{vc}) - \frac{\partial}{\partial z}(\overline{wc}) \qquad (1b)$$

This differential equation is three-dimensional and time dependent. Instead we will use a two-dimensional and time dependent model. Therefore, let us look at the lateral integrated concentration. Integrating equation (1b) over y gives us

$$\frac{\partial}{\partial t}\int_{-\infty}^{\infty} C\,dy + U\frac{\partial}{\partial x}\int_{-\infty}^{\infty} C\,dy + V\int_{-\infty}^{\infty}\frac{\partial}{\partial y}\,dy + W\frac{\partial}{\partial z}\int_{-\infty}^{\infty} C\,dy = -\int_{-\infty}^{\infty}\frac{\partial}{\partial y}\overline{vc}\,dy - \frac{\partial}{\partial z}\int_{-\infty}^{\infty}\overline{wc}\,dy \qquad (2a)$$

The third term on the left hand side and the first term on the right hand side vanish.

Substitute $\int_{-\infty}^{\infty} C\,dy = C_y$ which gives

$$\frac{\partial C_y}{\partial t} + U\frac{\partial C_y}{\partial x} + W\frac{\partial C_y}{\partial z} = -\frac{\partial}{\partial z}\int_{-\infty}^{\infty}\overline{wc}\,dy \qquad (2b)$$

The diffusion equation (1a) has now been reduced to a two-dimensional time dependent equation. To be able to solve this equation we have to know $\int_{-\infty}^{\infty}\overline{wc}\,dy$; the lateral integrated vertical flux. We will therefore introduce the differential equation for $\overline{wc}$

$$\frac{\partial\overline{wc}}{\partial t} + U\frac{\partial\overline{wc}}{\partial x} + V\frac{\partial\overline{wc}}{\partial y} + W\frac{\partial\overline{wc}}{\partial z} = -\overline{uw}\frac{\partial C}{\partial x} - \overline{vw}\frac{\partial C}{\partial y} - \overline{w}^2\frac{\partial C}{\partial y} + \frac{g}{\Theta_0}\overline{c\theta} - \frac{\partial}{\partial x}\overline{uwc} -$$

$$- \frac{\partial}{\partial y}\overline{vwc} - \frac{\partial}{\partial z}\overline{w^2c} - \frac{\overline{c}}{\rho_0}\frac{\partial\overline{p}}{\partial z} - \nu\overline{\frac{\partial w}{\partial x}\frac{\partial c}{\partial x}} - \nu\overline{\frac{\partial w}{\partial y}\frac{\partial c}{\partial y}} - \nu\overline{\frac{\partial w}{\partial z}\frac{\partial c}{\partial z}}\ . \qquad (3)$$

The three terms containing ν, the molecular diffusion terms, are negligible in atmospheric diffusion applications.

The term $\frac{\partial}{\partial x}\overline{uwc}$ is supposed to be much smaller than the advection term $U\frac{\partial\overline{wc}}{\partial x}$.

The pressure term $\frac{\overline{c}}{\rho_0}\frac{\partial\overline{p}}{\partial z}$ is parameterized according to Rotta-Launder:

$$\overline{\frac{c}{\rho_0}\frac{\partial p}{\partial z}} = \frac{1}{\rho_0}\frac{\partial\overline{cp}}{\partial z} - \alpha_1\frac{q}{\ell}\overline{wc} - \alpha_2\frac{q}{\Theta_0}\overline{c\theta} \qquad (4)$$

The terms $\frac{\partial}{\partial z}(\overline{w^2c}) + \frac{1}{\rho_0}\frac{\partial(\overline{cp})}{\partial z}$ are parameterized according to Donaldson(1973), Mellor (1973):

$$\frac{\partial}{\partial z}(\overline{w^2c}) + \frac{1}{\rho_0}\frac{\partial(\overline{cp})}{\partial z} = -A\cdot\frac{\partial}{\partial z}q\cdot\ell\frac{\partial\overline{wc}}{\partial z} \qquad (5)$$

where

q^2 is double the turbulence energy

ℓ is the turbulence length scale, taken from the wind model (Enger, 1983) and α_1, α_2 and A are constants.

Equation (3) can now be expressed accordingly:

$$\frac{\partial \overline{wc}}{\partial t} + U\frac{\partial \overline{wc}}{\partial x} + V\frac{\partial \overline{wc}}{\partial y} + W\frac{\partial \overline{wc}}{\partial z} = -\overline{uw}\frac{\partial C}{\partial x} - \overline{vw}\frac{\partial C}{\partial y} - \overline{w^2}\frac{\partial C}{\partial z} + \frac{g}{\Theta_0}(1-\alpha_2)\overline{c\theta} -$$

$$- \frac{\partial}{\partial y}\overline{vwc} + A\frac{\partial}{\partial z} q \cdot \ell \frac{\partial \overline{wc}}{\partial z} - \alpha_1 \frac{q}{\ell}\overline{wc} \qquad (6)$$

To get $\int_{-\infty}^{\infty} \overline{wc}dy$ we integrate (6) over y.

Equation (6) is then reduced to

$$\frac{\partial \overline{wc}_y}{\partial t} + U\frac{\partial \overline{wc}_y}{\partial x} + W\frac{\partial \overline{wc}_y}{\partial z} = -\overline{uw}\frac{\partial C_y}{\partial x} - \overline{w^2}\frac{\partial C_y}{\partial z} + \frac{g}{\Theta_0}(1-\alpha_2)\int_{-\infty}^{\infty}\overline{c\theta}dy +$$

$$+ A\frac{\partial}{\partial z} q \cdot \ell \cdot \frac{\partial \overline{wc}_y}{\partial z} - \alpha_1 \frac{q}{\ell}\overline{wc}_y \qquad (7)$$

where

$$\overline{wc}_y = \int_{-\infty}^{\infty} \overline{wc}dy$$

To solve this differential equation we have to know $\int_{-\infty}^{\infty}\overline{c\theta}dy$. We introduce the equation for $\overline{c\theta}$ as above for $\overline{wc}$. If we treat the terms in the equation for $\overline{c\theta}$ in a similar fashion to those in the equation for $\overline{wc}$ and then integrate over y, the equation for $\overline{c\theta}$ may be written

$$\frac{\partial \overline{c\theta}_y}{\partial t} + U\frac{\partial \overline{c\theta}_y}{\partial x} + W\frac{\partial \overline{c\theta}_y}{\partial z} = -\overline{u\theta}\frac{\partial C_y}{\partial x} - \overline{w\theta}\frac{\partial C_y}{\partial z} - \frac{\partial \Theta}{\partial z}\overline{wc}_y - \alpha_3\frac{q}{\ell}\overline{c\theta}_y + A\frac{\partial}{\partial z} q \cdot \ell \frac{\partial \overline{c\theta}_y}{\partial z} \qquad (8)$$

where

$$\overline{c\theta}_y = \int_{-\infty}^{\infty}\overline{c\theta}dy$$

Our system of equations (2), (7) and (8) can now be solved after determining the constants α_1, α_2, α_3 and A.

2.2 *The model coefficients*

We assume that the underlying surface is flat and homogeneous. Furthermore we assume that the concentration field is horizontally homogeneous and that stationary conditions apply. Under these assumptions the equations for $\overline{wc}$ and $\overline{c\theta}$ in the surface layer are reduced to

$$-\overline{wc} = \frac{\ell}{\alpha_1 q}\left(\overline{w^2}\frac{\partial C}{\partial z} - \frac{g}{\Theta_0}(1-\alpha_2)\overline{c\theta}\right) \qquad (9)$$

$$-\overline{c\theta} = \frac{\ell}{\alpha_3 q}\left(\overline{w\theta}\frac{\partial C}{\partial z} + \overline{wc}\frac{\partial \Theta}{\partial z}\right) \qquad (10)$$

In neutral conditions $\overline{c\theta} = 0$ as $\overline{w\theta} = 0$ and $\frac{\partial \theta}{\partial z} = 0$, accordingly equation (9) is reduced to

$$- \overline{wc} = \frac{\ell}{\alpha_1 q} \overline{w^2} \frac{\partial C}{\partial z} = K_z \frac{\partial C}{\partial z} \tag{11}$$

where

$$K_z = \frac{\ell}{\alpha_1 q} \overline{w^2}$$

According to Nieuwstadt and van Ulden (1977) $K_z = 1.35\ K_M = K_H$ which means that

$$\frac{\ell}{\alpha_1 q} \overline{w^2} = 1.35 u_* kz \tag{12}$$

Furthermore, we have according to measurements in the neutral surface layer, e.g. Enger (1983)

$$q^2 = B_1^{2/3} u_* \text{ , where } B_1 = 42.5 \tag{13}$$

$$\overline{w^2} = 1.7 u_*^2 \tag{14}$$

$$\ell = kz \tag{15}$$

Inserting these expressions in equation (12) we get $\alpha_1 = 0.36$. α_2 is simply set equal to zero (Donaldson, 1973).

According to Saab (1979) the diffusion coefficient A is about 1.0 and according to Enger (1983) the diffusion coefficient for the energy equation and for the temperature variance equation is equal to 1.0. We have also applied that value here for the second moments equations, i.e. A = 1.0. The model has also been tested regarding smaller values of A. If we use Yamada's and Mellor's (1975) value A = 0.23 we, however, get an unrealistic concentration field in the convective boundary layer.

α_3 has to be determined numerically by comparing the results from experiments, but we could get an idea of its magnitude by comparing it with the corresponding constant in the equation for the momentum equation for water vapor, $\overline{\theta r}$. According to Yamada and Mellor (1975) the differential equation for $\overline{\theta r}$ is

$$\frac{\partial \overline{\theta r}}{\partial t} - \frac{\partial}{\partial z} \left(\lambda_2 \frac{\partial}{\partial z} \overline{\theta r} \right) = - \overline{w\theta} \frac{\partial R}{\partial z} - \overline{wr} \frac{\partial \theta}{\partial z} - \frac{2q}{B_2 \ell} \overline{\theta r} \tag{16}$$

Comparing this equation with equation (8) we get

$\alpha_3 = \frac{2}{B_2}$ where $B_2 = 15.1$ if $B_1 = 42.5$ (Enger, 1983)

and where $B_2 = 8.0$ if $B_1 = 15.0$ (Mellor, 1973)

We will therefore test the model for different α_3-values between 0.1 and 0.3. As shown below $\alpha_3 = 0.17$ gives very satisfactory agreement with measurements.

2.3 *The gridsystem and the finite difference scheme*

The grid is equally spaced in the z-direction, with $\Delta z = 15$ m when testing the dispersion in a convective boundary layer and with $\Delta z = 5$ m in a stable boundary layer. In the x-direction the grid is also equally spaced, with $\Delta x = 200$ m and with the first grid point at 25 m from the source in the test of a convective boundary layer and the first grid point at 200 m from the source in the test of a stable stratification.

As shown in Enger (1983), Eq (7) and Eq (8) can be reduced to a general expression, namely

$$\frac{\partial \Phi}{\partial t} = \frac{\partial}{\partial z}\left(K \frac{\partial \Phi}{\partial z}\right) - R\frac{\partial \Phi}{\partial z} - P\Phi + F \qquad (17)$$

where Φ, K, R, P and F are given in Table 1.

Table 1. Identification of the variable Φ and the parameters K, R, P and F

	Φ	K	R	P	F
Eq (5)	$\overline{wc}_y$	$Aq\ell$	W	$\frac{\alpha_1 q}{\ell}$	$-U\frac{\partial \overline{wc}_y}{\partial x} - \overline{uw}\frac{\partial C_y}{\partial x} - \overline{w^2}\frac{\partial C_y}{\partial z} + \frac{g}{\Theta_0}\overline{c\theta}_y$
Eq (6)	$\overline{c\theta}_y$	$Aq\ell$	W	$\frac{\alpha_3 q}{\ell}$	$-U\frac{\partial \overline{c\theta}_y}{\partial x} - \overline{u\theta}\frac{\partial C_y}{\partial x} - \overline{w^2}\frac{\partial C_y}{\partial z} - \frac{\partial \Theta}{\partial z}\overline{wc}_y$

These two equation are solved with the aid of a finite difference scheme by Laasonen (Richtmyer et al, 1967)

$$\Phi_j^{n+1} + \Phi_j^n = \frac{\Delta t}{2(\Delta x)^2}\left\{(K_{j+1}^n + K_j^n)\Phi_{j+1}^{n+1} - (K_{j+1}^n + 2K_j^n + K_{j-1}^n)\Phi_j^{n+1} + \right.$$

$$\left. + (K_j^n + K_{j-1}^n)\Phi_{j-1}^{n+1}\right\} - \frac{R_j^n \cdot \Delta t}{2 \cdot \Delta z}(\Phi_{j+1}^{n+1} - \Phi_{j-1}^{n+1}) - \Delta t(P\Phi_j^{n+1} - F_j^n) \qquad (18)$$

The terms, $a\frac{\partial b}{\partial x}$, are approximated as

$$a\frac{\partial b}{\partial x} = a_{i,j}\frac{b_{i,j} - b_{i-1,j}}{\Delta x} \tag{19}$$

where the subscripts i and j represent the ith grid point in the x-direction and jth point in the z-direction.

n is the number of time steps from the start.

The equation for the integrated concentration, Eq (2), is solved according to the expression

$$C_{i,j}^{n+1} = C_{i,j}^{n} + \Delta t\left\{- U_j\frac{(C_{i+1,j}^{n} - C_{i,j})}{\Delta x} - W_j\frac{(C_{i,j+1} - C_{i,j-1})}{2\Delta z} - \right.$$

$$\left. - \frac{\overline{wc}_{i,j+1} - \overline{wc}_{i,j-1}}{2\Delta z}\right\}. \tag{20}$$

2.4 *Initial and boundary conditions*

To get an initial concentration field we determine the laterally integrated concentration, C_y, out of the Gaussian formula

$$C_y(x,z) = \frac{Q}{\sqrt{2\pi}\cdot\sigma_z(x)\cdot U(z_s)}\left\{\exp\left(-\frac{(z_s - z)^2}{2\sigma_z^2(x)}\right) + \exp\left(-\frac{(z_s + z)^2}{2\sigma_z^2(x)}\right)\right\} \tag{21}$$

where

$\sigma_z(x)$ is the vertical standard deviation at the distance x from the source

z_s is the effective source height

$U(z_s)$ is the wind at the source height

z is the height above the surface and

Q is the source strength

In a higher order closure model we can start our calculation near the source. We are not limited here to ground level sources or to large distances downstream the source as in K-theory. The validity of K-theory requires that the convective terms (those on the left-hand side of Eq (6)) and the diffusion term are negligible in comparison with the remaining terms. For a one-dimensional problem with neutral stability, Eq (6) is then reduced to

$$\overline{wc} = - \frac{\overline{w^2}\ell}{\alpha_1} \frac{\partial C}{\partial z} = - K \frac{\partial C}{\partial z}$$

This reduction is valid only under very special conditions and mostly other terms in Eq (6) are important. As the plume width is small near the source we want to use a use a Gaussian distribution in the two first grid points downstream the source, otherwise we have to use much more gridpoints in the vertical direction. To get the Gaussian distribution of the integrated concentration we have to determine σ_z, see section 2.5.

At the top of the model (see below) the concentration is set equal to zero. To get the concentration at the surface we look at Eq (2b) and Eq (7). Assuming stationary conditions, which means that the $\frac{\partial}{\partial t}$ -terms are equal to zero and $W = 0$, the equations (2b) and (7) are reduced to

$$U \frac{\partial C_y}{\partial x} = - \frac{\partial \overline{wc}_y}{\partial z} \tag{22}$$

$$U \frac{\partial \overline{wc}_y}{\partial x} = - \overline{uw} \frac{\partial C_y}{\partial x} - \overline{w^2} \frac{\partial C_y}{\partial z} + \frac{g}{\Theta_0} \overline{c\theta}_y - \frac{\alpha_1 q}{kz} \overline{wc}_y \tag{23}$$

At the surface ($z = 0$) we get $\left[\frac{\partial \overline{wc}_y}{\partial z} \right]_{z=0} = 0$ from Eq (22).

From Eq (23) we get

$$\overline{wc}_y = \frac{kz}{\alpha_1 q} \left[- \overline{uw} \frac{\partial C}{\partial x} - \overline{w^2} \frac{\partial C}{\partial z} + \frac{g}{\Theta_0} \overline{c\theta} - U \frac{\partial \overline{wc}}{\partial x} \right] \tag{24}$$

Differentiating this equation with respect to z leads to

$$\frac{\partial \overline{wc}_y}{\partial z} = \frac{k}{\alpha_1 q} \left[- \overline{uw} \frac{\partial C}{\partial x} - \overline{w^2} \frac{\partial C}{\partial z} + \frac{g}{\Theta_0} \overline{c\theta} - U \frac{\partial \overline{wc}}{\partial x} \right] +$$

$$+ \frac{kz}{\alpha_1 q} \left[- \overline{uw} \frac{\partial^2 C}{\partial x \partial z} - \overline{w^2} \frac{\partial^2 C}{\partial z^2} + \frac{g}{\Theta_0} \frac{\partial \overline{c\theta}}{\partial z} - \frac{\partial}{\partial z} U \frac{\partial \overline{wc}}{\partial x} \right] \tag{25}$$

For $z = 0$ we have $\overline{c\theta} = 0$, $U = 0$ and $\frac{\partial \overline{wc}_y}{\partial z} = 0$. Thus Eq (25) is reduced to

$$0 = - \overline{uw} \frac{\partial C}{\partial x} - \overline{w^2} \frac{\partial C}{\partial z} \tag{26}$$

As the lower boundary we get

$$\frac{\partial C}{\partial z} = -\frac{\overline{uw}}{\overline{w^2}}\frac{\partial C}{\partial x} = \frac{u_*^2}{1.7u_*^2}\frac{\partial C}{\partial x} = \frac{1}{1.7}\frac{\partial C}{\partial x} \tag{27}$$

As initial profiles for the moments $\overline{wc}_y$ and $\overline{c\theta}_y$ we have used guessed values, but the model itself will generate appropriate turbulence moments after a few minutes of integration time.

At the surface boundary, $z = 0$, we have $\overline{wc} = 0$ and $\overline{c\theta} = 0$

At the upper boundary ($z = 1500$ m for the convective case and $z = 1000$ m for the stable case, see below) we get

$$\frac{\partial \overline{wc}}{\partial z} = \frac{\partial \overline{c\theta}}{\partial z} = 0 \tag{28}$$

2.5 *Determination of the standard deviations*

An equation for the standard deviation, σ_y, of the cross wind spread of material which is released continuously from a point source, was derived by Taylor in 1921

$$\sigma_y^2 = 2\sigma_v^2 \int_0^t \int_0^{t_1} R_L(t_2)\,dt_2\,dt_1 \tag{29}$$

where

σ_v is the standard deviation of lateral turbulent velocity fluctuations

t is the travel time from the source to the receptor and

R_L is the Lagrangian auto correlogram for lateral turbulence.

Pasquill (1974) shows that this equation can be transformed, using the definition of a Lagrangian energy spectrum to the form

$$\sigma^2_{y_{T_s},t} = \sigma_v^2 \cdot t^2 \cdot \int_0^\infty F_L(n) \cdot \left(1 - \frac{\sin^2 \pi n T_s}{(\pi n T_s)^2}\right)\left(\frac{\sin^2 \pi n t}{(\pi n t)^2}\right) dn \tag{30}$$

where

T_s is the sampling time

t is the travel time from source to receptor

σ_v is the standard deviations of the local wind fluctuations, $\sqrt{\overline{v^2}}$

$F_L(n)$ is the normalized Lagrangian energy spectrum for $\overline{v^2}$ and

n is the frequency.

If we have to use an Eulerian spectrum instead Pasquill (1974) shows that the standard deviation of the crosswind spread can be obtained from

$$\sigma^2_{y_{T_s},t} = \sigma_v^2 \cdot t^2 \cdot \int_0^\infty F_E(n) \left(\frac{1 - \sin^2(\frac{\pi n T_s}{\beta})}{\left(\frac{\pi n T_s}{\beta}\right)^2} \right) \left(\frac{\sin^2(\frac{\pi n t}{\beta})}{\left(\frac{\pi n t}{\beta}\right)^2} \right) dn \qquad (31)$$

where

$F_E(n)$ is the normalized Eulerian energy spectrum for $\overline{v^2}$ and

β is the quotient between the Lagrangian time scale and the Eulerian time scale.

The sine terms in Eq (31) are filters that effectively block out turbulent fluctuations with time scales less than the travel time t and greater than the sampling time T_s. The sampling time T_s is usually chosen to be 1 h. According to Pasquill (1974) various theoretical estimates of the ratio $\beta = t_L/t_E$ all lead to $\beta = c/(\sigma_v/U)$ where c is a constant ranging from 0.35 to 0.8.

In neutral conditions $\beta \approx 4$. In all our tests we have used this β-value.

We will use Eq (31) to calculate the vertical standard deviation σ_z and the crosswind standard deviation σ_y of the spread of material from a point source. We only need the σ_z-values to calculate the initial values of the concentration profile. As we are solving the crosswind integrated concentration field with the numerical model we need the σ_y-values in order to get the lateral spread of the material.

First we want to get expressions for the Eulerian velocity spectra as functions of height and stability.

The Kansas measurements, Kaimal et al (1972), indicate similarity in shape for the stable spectra if normalized by their respective variance and expressed as a function of f/f_0, where

f_0 is the intercept of the extrapolated inertial subrange spectrum with the line $\frac{nE_\alpha(n)}{\overline{\alpha^2}} = 1$

$$\frac{nE_\alpha(n)}{\overline{\alpha^2}} = \frac{A\, f/f_0}{1 + A\cdot(f/f_0)^{5/3}} \qquad (32)$$

where

α = U, V, W or

n is the frequency

$f = \frac{n\cdot z}{U}$

U is the meanwind speed and

z is the height above the surface.

According to the Kansas measurements A takes the value of 0.164.

Caughey (1977) made measurements at higher levels in the stable baundary layer and for a greater range of stabilities. His spectra could be approximated with the same formula as for the Kansas spectra, but he got the constant A = 0.3.

If we accept the form above for the $\overline{w^2}$-spectra, Eq (32), we could theoretically determine the A-value.

By definition we have $\int_0^\infty \frac{E_w(n)}{\overline{w^2}}\,dn = \int_0^\infty F_w(n)\,dn = 1$ that means

$$1 = \int_0^\infty \frac{E_w(n)}{\overline{w^2}}\,dn = \int_0^\infty \frac{A\cdot\frac{1}{n}\cdot\frac{f}{f_0}}{1+A(\frac{f}{f_0})^{5/3}}\,dn = \int_0^\infty \frac{A\cdot\frac{1}{n}\cdot\frac{nz}{U}\cdot\frac{1}{f_0}}{1+A(n\,\frac{z}{U}\,\frac{1}{f_0})^{5/3}}\,dn = \frac{A^{2/5}}{5/3}\cdot\frac{\Gamma(\frac{3}{5})\cdot\Gamma(\frac{2}{5})}{\Gamma(1)} \qquad (33)$$

where $\Gamma(x)$ is the Gamma function

which gives us

A = 0.181

To get the spectra for different stabilities we have to know the variation of f_0 with stability. The relation between f_0 and f_m, where f_m is the value of the reduced frequency f at the spectral peak, is $f_0 = 0.26 f_m$ according to Kaimal (1973)

In Kaimal's (1973) Fig 3 f_0 is a function of z/L. We here approximate this dependence upon z/L for f_0 with

$f_0 = 0.26 \cdot 0.56(1 + 2z/L)$, $z/L \leq 3.3$

For z/L greater than 3.3 we have used a constant value $f_0 = 1.11$

In a convective boundary layer the w-spectrum (Caughey, 1982) takes the form

$$\frac{nE_w(n)}{w_*^2\psi^{2/3}} = 0.20f_i^{-2/3} \tag{34}$$

in the inertial subrange

where

n is the frequency

f_i is the dimensionless frequency $\frac{nz_i}{U}$

z_i is the height of the convective boundary layer

E_w is the energy spectrum for W

$w_* = (Q_0 z_i g/\Theta_0)^{1/3}$ is the scaling velocity for a convective boundary layer and

ψ is the dimensionless dissipation rate $\frac{\varepsilon\Theta_0}{gQ_0}$.

At lower frequencies the curves for the normalized spectra separate as a function of z/z_i.

We want to fit the experimental normalized spectra for the convective boundary layer with an analytical expression. We have supposed this expression takes the following form.

$$Y = \frac{nE_w}{w_*^2 \cdot \psi^{2/3}} = \frac{0.2 \cdot f_i^{-2/3}}{1 + c(f_i)^{-b}} \tag{35}$$

At the spectral peak $\frac{dY}{df_i} = 0$ which gives us

$$c = \frac{f_{max}^{b}}{\frac{3}{2}b - 1} \tag{36}$$

According to Caughey (1982) the f_{max}-profile could be approximated as

$$f_{max} = 1/[1.76 \cdot (1 - \exp(-4z/z_i)) - 0.0003\exp(8z/z_i)] \tag{37}$$

when $0.1 \leq \frac{z}{z_i} < 1$.

We have accepted this form in this model when $0.2 \leq \frac{z}{z_i} < 1$ and for the region $z/z_i < 0.2$ we have chosen the form

$$f_{max} = 0.223 \cdot (z/z_i)^{-0.917} \quad \text{(see Fig 1)} \tag{38}$$

In Fig 2 we have plotted the normalized spectra according to Eq (35) with

$$b = -0.056 \ln(z/z_i) + 1.234 \tag{39}$$

As can be seen in Fig 2 this form of the normalized spectra fits the measured spectra quite well.

The dimensionless vertical velocity variance, σ_w^2/w_*^2, can be obtained from Eq (35) by integrating over all frequencies

$$\frac{\sigma_w^2}{w_*^2} = \psi^{2/3} \cdot 0.20 \cdot \int_0^\infty \frac{(\frac{z_i}{U})^{-2/3} \cdot n^{-5/3}}{1 + \frac{f_{max}^b}{\frac{3b}{2}-1} (\frac{U}{z_i})^b \cdot n^{-b}} dn = 0.20\psi^{2/3} \cdot \frac{(\frac{3b}{2}-1)^{\frac{2}{3b}} \cdot f_{max}^{-2/3} \cdot \frac{\pi}{b}}{\sin(\frac{2}{3b}\pi)} \tag{40}$$

We get the equation for the standard deviation σ_z of the vertical spread of material from a point source from

$$\sigma_z^2 = \overline{w^2} \cdot t^2 \cdot \int_0^\infty F(n) \frac{\sin^2(\frac{\pi n t}{\beta})}{(\frac{\pi n t}{\beta})^2} dn \ . \tag{41}$$

In order to be able to integrate Eq (41) analytically we must approximate the filter function $\sin^2(\frac{\pi n t}{\beta})/(\frac{\pi n t}{\beta})^2$ with another function.
For the stable boundary layer we have chosen the function $\frac{1}{1 + \frac{1}{6.5}(\frac{\pi n t}{\beta})^5}$

Equation (32) and this expression for the filter function in Eq (41) give us

$$\sigma_z^2 = \overline{w^2} \cdot t^2 \cdot \int_0^\infty \frac{A \ f/f_0 \cdot \frac{1}{n}}{1 + A \ f/f_0} \cdot \frac{1}{1 + \frac{1}{6.5}(\frac{\pi n t}{\beta})^5} dn =$$

$$= \overline{w^2} \cdot t^2 \cdot \frac{3}{5} \cdot A^{2/5} \cdot \frac{\pi}{\sin(\frac{3}{5}\pi)} \left(\frac{1}{1-B^3} + \frac{B^{2/5}}{3(B-1)} + 2C \cdot (D\cos\frac{2}{5} + E\sin\frac{2}{5}\pi) \right) \tag{42}$$

where

$A = 0.181$

$B = \left[\left(\frac{t \cdot uf_0}{z \cdot \beta} \right)^5 \cdot A^{-3}/6.5 \right]^{1/3}$

$C = 1/3(2B)^{2/5}/(B^2 + B + 1)$

$D = 0.5(5 + B)$

$E = -\sqrt{3}$ and

$\overline{w^2}$ is obtained from the numerical wind model (Enger 1983).

The expression $\frac{3}{5}A^{2/5} \cdot \frac{\pi}{\sin(\frac{3}{5}\pi)}$ in Eq (42) is equal to 1.

For the convective boundary layer we have used another filter function namely

$$\frac{1}{1+\frac{1}{4}(\frac{\pi n t}{\beta})^{3b}}$$

where b is obtained from Eq (39).

In Eq (41) F(n) is the power spectrum function normalized with σ_w^2. As we get $\overline{w^2}$ from the windmodel we have to normalize the absolute spectrum function, $E_w(n)$, in Eq (35) with σ_w^2 from Eq (40). This also means that we will get rid of the problem of determining the ψ-function.

The filter function and the normalized spectrum function from Eq (35) and Eq (40) in Eq (41) give us

$$\sigma_z^2 = \overline{w^2} \cdot t^2 \cdot \frac{\sin(\frac{2}{3b})}{(\frac{3b}{2}-1)^{\frac{2}{3b}} \cdot f_{max}^{-2/3} \cdot \frac{\pi}{b}} \int_0^\infty \frac{f_i^{-2/3} \cdot \frac{1}{n}}{1+\frac{1}{\frac{3}{2}b-1}(\frac{f}{f_{max}})^b} \cdot \frac{1}{1+\frac{1}{4}(\frac{\pi n t}{\beta})^{3b}} dn =$$

$$= \overline{w^2} \cdot t^2 \cdot \left(\frac{1}{1-B^3} + \frac{B^{\frac{2}{3b}}}{3(B-1)} + 2C \cdot (D \cdot \cos(\frac{2}{3}(1-\frac{2}{3b})\pi)) + E \cdot \sin(\frac{2}{3}(1-\frac{2}{3b})\pi) \right) \quad (43)$$

where

$$B = \left(\frac{\pi \cdot t \cdot U \cdot f_{max}}{z_i \cdot \beta} \right)^b \cdot 4^{-1/3} \cdot (\frac{3}{2}b - 1)^{-1}$$

$C = \frac{1}{3}(2\ B)^{\frac{2}{3b}} / (B^2 + B + 1)$

$D = 0.5\ (5 + B)$ and

$E = -\sqrt{3}$.

The crosswind standard deviation, σ_y, is derived in the same manner as σ_z. In stable stratification the Eulerian energy spectrum for $\overline{v^2}$ is given by Eq (32).

For the $\overline{v^2}$-spectra we have assumed that the dependence on z/L of $f_0 = 0.26 f_{max}$ is

$f_0 = 0.26 \cdot 0.24(1 + 1.8z/L)$ $\quad 0 \leq z/L \leq 3$

$f_0 = 0.40$ $\quad z/L > 3$

according to measurements of f_{max} (Kaimal et al, 1972)

We get σ_y^2 from Eq (42) by exchanging $\overline{w^2}$ with $\overline{v^2}$ and using f_0 above.

In the convective boundary layer we use the same shape of the spectra as for the energy spectra for W, Eq (35), but with

$b = 4/3$

$f_{max} = 9.1 \cdot 10^{-2}(\frac{z}{z_i})^{-0.647}$ $\quad z/z_i \leq 0.05$

$f_{max} = 0.63$ $\quad z/z_i > 0.05$

In Fig 3 we see that this form of the spectra fits the measured spectra (Kaimal et al, 1976) quite well.

The crosswind standard deviation for a plume, σ_y, we now get from (Eq 43) by exchanging $\overline{w^2}$ with $\overline{v^2}$ and using these new b and f_{max} values.

When looking at the crosswind standard deviation we also have to take into consideration the spread caused by the 'synoptic' wind spectra. According to Hess and Clarke (1973) the synoptic spectra between 1 and 10 cycles per day is proportional to $n^{-2.4}$. Smedman-Högström and Högström (1975) show that the synoptic part of the spectra is stability dependent. We have approximated this stability dependence accordingly:

$$\frac{E_s(n)}{\sigma_v^2} = \frac{1}{n}(\frac{f}{f_0})^{-1.4} \cdot 10^{-3} \qquad z/L \leq 0.05 \qquad (44a)$$

$$\frac{E_s(n)}{\sigma_v^2} = \frac{1}{n}(\frac{f}{f_0})^{-1.4} \cdot 2 \cdot 10^{-2} z/L \qquad 0.05 < z/L < 1 \qquad (44b)$$

$$\frac{E_s(n)}{\sigma_v^2} = \frac{1}{n}(\frac{f}{f_0})^{-1.4} \cdot 2 \cdot 10^{-2} \qquad z/L \geq 1 \qquad (44c)$$

Instead of using a filterfunction when integrating these spectra to obtain the synoptic part of the standard deviation we integrate equation (44) from β/T_s to β/t getting

$$\sigma_{y_c}^2 = \overline{v^2} \cdot t^2 \int_{\beta/T_s}^{\beta/t} \frac{E_s(n)}{\sigma_v^2} dn \qquad (45)$$

The total crosswind standard deviation for spread from a point source is then

$$\sigma^2_{y_{tot}} = \sigma^2_y + \sigma^2_{y_c} \qquad (46)$$

Especially is a stable stratified boundary layer the effect of wind shear on the horizontal spread can be considerable. According to Smith (1965) the cross-wind spread at a given level after time t could be expressed in three terms:

$$\sigma^2_y(t,z) = \sigma^2_v t^2 \int_0^\infty F_L(n)\left(\frac{\sin \pi nt}{\pi nt}\right)^2 dn + \frac{1}{4}\sigma^2_w \left(\frac{\partial V}{\partial z}\right)^2 t^4 \int_0^\infty G_L(n)\left(\frac{\sin \pi nt - \pi nt \cdot \cos \pi nt}{(\pi nt)^2}\right)^2 dn -$$

$$- \left(\frac{\overline{vw}}{\sigma_w}\right)^2 t^2 \int_0^\infty G_L(n) \left(\frac{\sin \pi nt}{\pi nt}\right)^2 dn \qquad (47)$$

$F_L(n)$ is the normalized Lagrangian spectrum for the crosswind spectrum

$G_L(n)$ is the normalized Lagrangian spectrum for the vertical component

The first term on the right hand side in the equation is equivalent to Eq (30) and is the direct effect of the horizontal component of turbulence.

The second term is the effect of the systematic wind shear and the third term on the right hand side is the effect of that part of the horizontal component which is correlated with the vertical component.

This last term acts in opposition to the second term. These two last terms can be handled in the same manner as the first one, see above. In the tests performed the wind-shear, however, is so small that these two last terms in Eq (47) can be excluded.

3 RESULTS

First we want to compare the results we get from simulations with the present model in a convective boundary layer with those of Willis' and Deardorff's tank experiments and Lamb's Lagrangian model (1978 and 1982).

Willis and Deardorff have made three water-tank experiments: one with a source near the surface (Deardorff and Willis, 1975), one with a source at level $0.25z_i$, where z_i is the height of the convective boundary layer (Willis and Deardorff, 1978) and one with a source in the middle of the convective mixing layer (Willis and Deardorff, 1981). From these tank experiments and from Lamb's model it was found that if we have a ground level source the centerline of a ground-level plume first moves parallel with the surface and then starts to rise rather rapidly. Willis and Deardorff (1975) show with their tank experiment that the ground-level plume began to rise after a travel time of about $0.5z_i/w_*$ or at a distance of about $0.5z_iU/w_*$. It reached an elevation of about $0.75z_i$ after a travel time of order z_i/w_*, Fig 11a. But at the same time for an elevated source both Willis' and Deardorff's tank experiments and Lamb's model revealed that the elevated plume centerline was descending until it intercepts the ground. These findings are grossly out of line with a conventional Gaussian model of diffusion. Discussions have been made if a higher order closure Eulerian model, as the present model, should be able to predict the ascending and descending of the plume in a convective boundary layer or not, see e.g. Lamb (1982).

Our set of equations to be used testing its application on despersion in a convective boundary layer is

$$\frac{\partial C_y}{\partial t} + U\frac{\partial C_y}{\partial x} + W\frac{\partial C_y}{\partial z} = -\frac{\partial \overline{wc}_y}{\partial z}$$

$$\frac{\partial \overline{wc}_y}{\partial t} + U\frac{\partial \overline{wc}_y}{\partial x} + W\frac{\partial \overline{wc}_y}{\partial z} = -\overline{uw}\frac{\partial C_y}{\partial x} - \overline{w^2}\frac{\partial C_y}{\partial z} + \frac{g}{\Theta_0}(1-\alpha_2)\overline{c\theta}_y + A\frac{\partial}{\partial z} q\ell \frac{\partial \overline{wc}_y}{\partial z} - \alpha_1 \frac{q}{\ell}\overline{wc}_y$$

$$\frac{\partial \overline{c\theta}_y}{\partial t} + U\frac{\partial \overline{c\theta}_y}{\partial x} + W\frac{\partial \overline{c\theta}_y}{\partial z} = -\overline{u\theta}\frac{\partial C_y}{\partial x} - \overline{w\theta}\frac{\partial C_y}{\partial z} - \frac{\partial \Theta}{\partial z}\overline{wc}_y + A\frac{\partial}{\partial z} q\ell \frac{\partial \overline{c\theta}_y}{\partial z} - \alpha_3 \frac{q}{\ell}\overline{c\theta}_y$$

where the constants are

$A = 1.0$

$\alpha_1 = 0.36$ and

$\alpha_2 = 0$.

α_3 has to be determined.

Let us suppose that we have a horizontal homogeneous surface so that the wind, temperature and their moments could be determined from a one dimensional model giving $W = 0$. We want to test the diffusion model for the convective boundary layer of the Wangara experiment DAY 33 at 1500 (Clarke et al, 1971). At that time the convective boundary layer was fully developed with $z_i = 1200$ m. We get the wind, the temperature and the turbulent quantities from a numerical model, (Enger, 1983). The quantities have been transformed into a coordinate system with the x-axis in the mean wind direction. The profiles used for wind, temperature and turbulent quantities are shown in Figs 4 - 8. First we will test the model with the source in the middle of the convective boundary layer. Chosing a too large value of α_3 ($\alpha_3 = 0.30$) we get a too slow descending of the plume and if we take a too small α_3-value ($\alpha_3 = 0.10$) the process is moving too rapidly. We have chosen $\alpha_3 = 0.17$, giving a development similar to Lamb's model and Willis and Deardorff's experiment for a source at half the height of the mixing layer. This α_3-value has been used for all the other simulations.

Figs 9a - 9d show the results for source heights, z_s, equal to $0.025z_i$, $0.25z_i$, $0.5z_i$ and $0.75z_i$ respectively. These figures should be compared with Lamb's results, Figs 10a - 10d, and Willis' and Deardorff's results, Figs 11a - 11c.

For a 'ground level release' (in this case we have $z_s = 0.025z_i$ which means that for $z_i = 1200$ m $z_s = 30$ m) the maximum centerline, Fig 9a, starts to rise at a distance of about $0.5 \frac{z_i u}{w_*}$ (which in this case is about 770 m from the source) up to an elevation of about $0.8z_i$. This is in very good agreement with the results from Deardorff's and Willis' tank experiment for a source height of about $0.067z_i$, Fig 11a.

The calculated crosswind integrated concentrations, C_y, for a source at the height $z_s = 0.25z_i$ are shown in Fig 9b. Here can be noted that the maximum concentration centerline descends until it intercepts the ground at a distance of about $0.5z_i u/w_*$. This is in very good agreement with Lamb's result. Between $0.6z_i u/w_*$ and $1.7z_i u/w_*$ the simulations with the present model give two maxima in the crosswind integrated concentration field, one ground level maximum and one elevated weak maximum at about $0.6z/z_i$. Beyond $1.7z_i u/w_*$ only this elevated maximum is left. According to Willis' and Deardorff's tank experiment the maximum concentration centerline intercepts the ground at about $0.4z_i u/w_*$ and then

starts to rise at about $0.9z_i u/w_*$ up to an elevation of about $0.7z/z_i$. Willis and Deardorff (1981) noted that the pronounced rebound of the plume centerline they observed was partly due to the small positive buoyancy their tracer acquire with time, but they found no evidence that this was the sole cause of the rebound. It is difficult to say if there are significant deficiencies in the numerical or laboratory models but Lamb's numerical Lagrangian solution of the dispersion gives the same result as the present model and as his model solves the dispersion in a quite different way it causes us to believe that such a pronounced rebound is dependent on the experimental set up.

For a source height $z_s = 0.5z_i$, Fig 9c, the plume is descending and intercepting the surface at a distance $0.9 \frac{z_i u}{w_*}$ from the source. The intercept occurs at about the same distance as Lamb got with his model. According to Willis' and Deardorff's experiment (Fig 11c) this distance is about $0.8 \frac{z_i u}{w_*}$. Also, in this case Willis and Deardorff got a pronounced rebound of the plume.

We have the same behaviour for a source at height $0.75z/z_i$, Fig 9d. The descending plume centerline intercepts the surface at a distance about $1.7 \frac{z_i u}{w_*}$, Fig 10d.

In Fig 12 the calculated dimensionless cross-wind integrated concentration at ground level $\frac{C_y(x,0)z_i u}{Q_0}$, for a ground level release, is compared with the Praire Grass data (Niuwstadt, 1980), with results from a water-tank experiment (Deardorff and Willis, 1975) and with Lamb's numerical model (Lamb, 1980). The present model result with $a_1 = a_2 = 0.17$ is in much better agreement with the Praire grass data then Lamb's model or Deardorff's and Willis' tank experiment. The ground level concentration for a ground level release is very sensitive to the constants a_1 and a_2. If we use $a_1 = a_2 = 0.20$ instead in our model the results coincide more with Lamb's and Willis' and Deardorff's results. But as it is difficult to explain the faster rate of decline in the measured concentrations by loss of tracer material for example in the field experiment (Barad and Haugen, 1959) we believe the atmospheric experiment data to be quite correct.

Let us now look at the ground level concentration in the center of the plume, $C(x,0,0)$ for elevated sources. First we want to make the concentration nondimensional by multiplying with $\frac{z_i z_s u}{Q_0}$ as Lamb (1982) and plot this nondimensional concentration against the nondimensional distance $\frac{xw_*}{z_s u}$, Fig 13. Lamb found the maximum nondimensional ground level concentration to be independent of release height. This is not confirmed by our calculations - instead we found it to vary between 0.6 and 1.3. We will therefore try another scaling. Let us use $z_s z_i (\frac{xw_*}{z_s u})_{max}$ rather than $z_s z_i$ to non-dimensionalize $C(x,0,0)$. This scaling is used in Fig 14 and we note that the maximum non-dimensionalized concentrations are roughly equal to 1.1.

The vertical standard deviation, σ_z, of the spread of material is used only for initialisation of the concentration field and for determining the cross wind integrated concentration at the upstream boundary. The σ_z-values are calculated from spectra, see Section 2.5. In Fig 15 we have compared the σ_z-values calculated in this way with experimentally determined standard deviations (Högström, 1964) during neutral conditions. We note from the figure that there is generally quite good agreement.

As stated earlier we assume a Gaussian distribution for the horizontal cross wind direction to exist. Deardorff and Willis (1975) found from their tank experiments that the lateral distribution of the concentration was indeed closely Gaussian. Measurements in the atmosphere also show that there is no systematic departure from a Gaussian distribution (Pasquill, 1974). The cross wind standard deviation is determined from spectra, see section 2.5. In Fig 16 we have compared our calculated σ_y-values for the release height $z_s = 0.025z_i$ with Prairie Grass data (Nieuwstadt, 1980), with Lamb's model results (Lamb, 1982) and with Deardorff's and Willis' water-tank experiment and we note that the present model calculations are in good agreement with both Prairie Grass data and Lamb's model results. For a source height at $0.25z_i$ the trend of the standard deviation with distance is in good agreement with both Willis' and Deardorff's experiments (1978) and Lamb's model results (1982), but the present model simulates about 10 % higher cross wind standard deviations, Fig 17.

In stable air the Gaussian assumption for the vertical concentration distribution is generally better than for the convective case, mainly because of the limited vertical extension of the plume (cf. Pasquille, 1974, p 203). We will therefore test the numerical model prediction for a stable case with the corresponding prediction based on the Gaussian assumption for the vertical distribution. The meteorological situation for the test is Wangara DAY 34 0100 h (Clarke et al., 1971) and the corresponding wind- and turbulence field has been generated with the boundary layer model of the present author (Enger, 1983). Cross-wind integrated concentrations for the release at 30 m have been generated in two ways:

1) With the Gaussian equation, Eq (21), over the entire range of distances, σ_z being determined by Eq (41) as described in the text.

2) With the numerical dispersion model, Eqs (2b), (7) and (8). The Gaussian profile has only been used for the upstream boundary (cf. section 2.4). As an initial concentration field we have tested both a Gaussian distribution and a non-Gaussian distribution giving the same results.

The results for two distances, 700 m and 1500 m, are presented in Figs 18 and 19 respectively. For both distances the agreement between the two methods is remarkably good. The implication of this is two-fold, namely that during stable conditions our model results show that the distribution is close to Gaussian and indicate that the vertical standard deviation has been correctly determined (cf. section 2.5).

We have also made a simulation of dispersion in a case with horizontally heterogenous conditions. It will represent island fumigation of the plume from an elevated point source situated on an upwind coast line. The following assumptions have been made:

1. The source is situated on the coast line at a height of 100 m.
2. The distance between the source and the island is 2 km.
3. The geostrophic wind is supposed to be constant with $U_g = 5$ m/s and $V_g = 0$ m/s.
4. Initially the potential temperature increases linearly with height, $\Theta = 275 + 0.0045z$.
5. The temperature at the lowest grid point at the upstream boundary is supposed to be stationary $\Theta_1 = 275^{o}$ K.
6. The temperature at the lowest grid point at the downstream boundary (on the island) is supposed to increase linearly with 1.5 ^{o}C per hour the first five hours then it is kept constant.
7. The roughness length for the sea is 0.00025 m and for the island 0.1 m.

The simulated wind, temperature and turbulencefields, after six hours integration time with the numerical wind model (Enger, 1983), are used as input in the dispersion model. The simulated wind, temperature and heat flux are shown in Figs 20 - 22. The dispersion model has been used to simulate this case and, for comparison, we have also simulated a case with no island.

The simulated cross wind integrated concentration field for the two cases, without and with an island, are shown in Figs 23a and 23b respectively. We note from these figures that the convective internal boundary layer over the island causes the plume to fumigate. In this case the maximum ground concentration appears about 2.5 km inland of the island. The result from this simulation seems reasonable.

Finally we want to verify the model simulations against data from a tracer experiment (S. Gryning et al., 1983). A tracer (SF_6) was released at a height of

95 m at the nuclear power station Barsebäck in southern Sweden, situated at the eastern coast line of Öresund. Tracer sampling units were placed in Copenhagen, Denmark, in two semi circles, one very close to the water front and the other about 3.5 km inland. The distance between the release point and the first semi circle of sampling units was about 21 km. Measurements of temperature, wind-speed and direction were carried out at several places in meteorological towers and with the help of radiosondes and pilot balloons. The locations of sampling sites and meteorological measurement sites are shown in Fig 24.

The dispersion experiment was carried out on June 23, 1982. Samples of the tracer were taken between 1048 - 1218 EMT. Simulations of the meteorological situation during the experiment have been done with the boundary layer model of the present author (Enger, 1983). As input for that model the geostrofic wind components are needed. During the experiment pilot balloon measurements were carried out at Jaegersborg, Denmark to get the wind-speed and wind direction. There was one launch at 0600 EMT and one at 1800 EMT. In our simulations we have supposed that the geostrofic wind above 500 m can be approximated with the measured wind. Unfortunately there were no wind measurements during the dispersion experiment. Therefore we simply approximate the geostrofic wind with a straight line between the measured wind profile above 500 m at 0600 EMT and at 1800 EMT and then extrapolate this line down to the surface, Fig 25. The geostrofic wind direction has been approximated in the same manner from the pilot balloon measurements at 0600 EMT and at 1800 EMT, Fig 26.

Radiosonde launches were performed at Jaegersborg at 1054 EMT and at 1205 EMT to get the temperature profiles, Fig 27. We have made our simulations with both these temperature profiles. We have furthermore supposed that the temperature at 1 m (the first grid point) is 12.5 ^{o}C during the experiment according to measurements on the island of Saltholm and at Avedøre, Fig 28.

A surface roughness length of 0.2 m has been used for grid points in open country in Sweden. Over the water between Sweden and Denmark a length of 0.00024 m has been used and in Denmark, Copenhagen, a supposed roughness length of 0.8 m has been used. The distances between grid points are set to 1000 m. We used 3 grid points in Sweden, 21 grid points over the waters and 6 grid points in Denmark.

To get the concentration at the upstream boundary we have used the Gaussian approximation, see section 2.4. The wind-speed at the source height, $u(z_s)$, in Eq (21) is taken as the measured wind-speed at Barsebäck, 11.5 m/s.

The cross wind standard deviation is solved according to section 2.5 up to the

coast of Denmark. At the Danish coast we get a drastic change in the lateral wind energy component. The cross wind standard deviation from the coast of Denmark and forward is solved with Eq (46) except that

$$\sigma_{y_c}^2 = t^2 \int_{\beta/T_s}^{\beta/t} \left(\frac{x_c}{x} \left[\frac{E_s(n)}{\sigma_v^2} \right]_{x_c} \overline{v^2(x_c)} + \frac{x-x_c}{x} \left[\frac{E_s(n)}{\sigma_v^2} \right]_x \overline{v^2(x)} \right) dn \qquad (48)$$

and

$$\sigma_y^2 = t^2 \int_0^{\infty} \left(\frac{x_c}{x} \overline{v^2(x_c)} [F(n)]_{x_c} + \frac{x-x_c}{x} \overline{v^2(x)} [F(n)]_x \right) \frac{\sin^2 \frac{\pi n t}{\beta}}{\left(\frac{\pi n t}{\beta} \right)^2} dn \qquad (49)$$

where

x_c is the distance between the point source and the Danish coast,

$[\ ]_{x_c}$ is the value of the parameter within the brackets at the distance x_c and

x is the actual distance from the point source, $x > x_c$.

Fig 29 shows the simulated wind profiles at three distances from the source, one corresponding to the wind conditions at Barsebäck, one at Saltholm and one at Avedøre. In the same figure we have plotted measured values of the wind-speeds at these sites. The boundary layer model seems to underestimate the wind-speed about 1.5 m/s. The cause of this is probably due to having used a too small geostrofic wind.

Model simulations of the ground level concentrations at the sampling sites are shown in Figs 29 and 30. We note from these figures that the model can simulate the concentration distribution very well. We can also note that the concentration is very much dependent on the stability. The temperature profile from the sounding at 1054 EMT gives weak stable conditions in the surface layer ($L = 200$) and the temperature profile at 1205 EMT gives near neutral conditions ($L = \infty$). The calculations show also that the crosswind standard deviation mostly depends on the 'synoptic' part of the spectra at the sampling sites' distances.

In Fig 31 we have plotted the ground level concentration in the center of the plume, $C(x,0,0)$ and we note that the maximum concentration lies about 4 km downstream the source. At the sampling sites' distances the maximum ground level concentrations are very well simulated.

SUMMARY AND CONCLUSIONS

A numerical higher order closure dispersion model is derived to simulate dispersion from a point source during various meteorological conditions. The model requires the solution of the lateraly integrated diffusion equation and the partial differential equation for the vertical turbulent flux of pollutant and for the covariance between temperature and concentration. The mean wind profiles and turbulence quantities are taken from a second order closure atmospheric boundary layer model developed by the auther (Enger, 1983). For the simulations of dispersion in a convective boundary layer simulated mean winds and turbulence quantities of the Wangara experiment DAY 33 at 1500 h have been used. At that time the convective boundary layer was fully developed. To be able to compare our simulations with laboratory experimental results, they have been normalized according to Deardorff (1975). Discussions have been made in the litterature whether an Eulerian diffusion model would enable the prediction of dispersion in a convective boundary layer or not. Willis' and Deardorff's laboratory experiments and Lamb's Lagrangian model have shown that for a ground level source the centerline of the lateral integrated concentration of the plume first moves parallel with the surface and then starts to rise rather rapidly. A plume from an elevated source, on the other hand, has been shown to descend to the ground during the same conditions.

When parameterizing the third order moments in the equations for the vertical turbulent flux of pollutant and for the covariance between temperature and concentration one gets constants that have to be determined. All constants but one are determined from surface layer data. The magnitude of the remaining one was determined, but it turned out that the simulation results were sensitive to the exact value of this constant. We have therefore determined this by simulating the dispersion from a point source in the middle of the convective boundary layer for various constant values and compared our results with Willis' and Deardorff's laboratory experimental result for a source at the same height. The plume centerline descended too slowly if a too large constant value was used and with a too small value the process moved too rapidly. The constant value giving the best result agreement with Deardorff's experiment has been used for all the other simulations. The results from these simulations show very good agreement with Willis' and Deardorff's experiments and with Lamb's model.

The lateral dispersion in the model is handled with a Gaussian approach, a procedure well supported by numerous atmospheric measurements as well as by

Willis' and Deardorff's laboratory experiments. The standard deviations are obtained from model generated standard deviations of the lateral wind component using Taylor's expression and Eulerian spectra. The quotient between the Lagrangian and Eulerian time scales, β, is set to 4.0. The Eulerian velocity spectra have been taken from recent literature. The model results obtained are shown to be in very good agreement with measurements.

In the above simulations a one-dimensional version of the wind model (Enger, 1983) has been applied which means that the streamwise variations in the meteorological fields have been neglected. The present model has, however, also been tested with these effects included. One simulated situation can be characterised as follows. An elevated source at a coast line emits pollutants into a stable marine boundary layer. After some travel distance the plume encounters an island where a convective boundary layer is being developed, and the plume fumigates. Our model seems to simulate this situation quite realistically.

A very similar situation has been tested against tracer experiment data. In that experiment a tracer was emitted from a point source at the coast line of Skåne in southern Sweden. After about 20 km travel distance the plume encounters the coast line of Denmark. Samples were taken at the Danish coast and along a semi circle about 3.5 km inland. During the experiment the atmosphere in the lowest hundred meters was near neutral or weak stable stratified. The simulations with the present model show very good agreement with the measured concentrations. The model seems to simulate very well both the cross wind integrated concentration and the cross wind standard deviation.

ACKNOWLEDGEMENTS

This work has been carried out in partial fulfilment of the degree of Doctor of Philosophy. It has been sponsored by the National Swedish Environment Protection Board (SNV 7-306178). The Öresund tracer experiment data have been acquired by Studsvik Energiteknik AB and they have kindly put them to my disposal.

I wish to thank the many colleagues and members of the technical staff at the Department of Meteorology, Uppsala, who have been very helpful during the various stages of this work. I will especially express my sincere thanks to my supervisor Professor Ulf Högström for fruitful discussions and advice.

REFERENCES

Barad, M.L. and Haugen, D.A., 1959: *A preliminary evaluation of Sutton's hypothesis for diffusion from a continuous point source.* J. Appl. Meteor., 16, 12-20.

Berlyand, M.E., Editor, 1971: *Air Pollution and Atmospheric Diffusion.* Israels Program for Scientific Translations. 220 pp.

Caughey, S.J., 1977: *Boundary layer turbulence spectra in stable conditions.* Boundary-Layer Meteorol., 11, 3-14.

Caughey, S.J., 1982: *Observed characteristics of the atmospheric boundary layer,* in: Atmospheric turbulence and air pollution modelling, F.T.M. Nieuwstadt and H. van Dop, Editors. D. Reidel Publishing Company, Dodrecht, Holland, 107-158.

Clarke, R.H., Brook, R.R., Reid, D.G. and Troup, A.J., 1971: *The Wangara Experiment: Boundary layer data.* Tech. Paper 19. Div. Meteor, Phys., CSIRO, Australia.

Deardorff, J.W. and Willis, G.E., 1975: *A parameterization of Diffusion into the mixed layer.* J. Appl. Meteor., 14, 1451-1458.

Donaldson, C. du P., 1973: *Construction of a dynamic model of the production of atmospheric turbulence and the dispersal of atmospheric pollutants.* In Workshop on Micrometeorology, D.A. Haugen, ed. American Meteorological Society Publication, 392 pp.

Enger, L., 1983: *Numerical boundary layer modeling with application to diffusion. Part 1: A two dimensional higher order closure model.* Department of Meteorology, University of Uppsala, Sweden, Report No 70.

Gryning, S-E., Lyck, E. and Widemo, U., 1983: *A tracer investigation of the atmospheric dispersion in the Öresund region.* Data and Technical report. Studsvik Energiteknik AB, Sweden. 83/NW-83/452.

Hess, G.D. and Clarke, R.H., 1973: *Time spectra and cross-spectra of kinetic energy in the planetary boundary layer.* Quart. J. Roy. Meteor. Soc., 99, 130-153.

Högström, U., 1964: *An experimental study of atmospheric diffusion.* Tellus 16, 205-251.

Kaimal, J.C., Wyngaard, J.C., Izumi, Y. and Coté, O.R., 1971: *Spectral characteristics of surface layer turbulence.* Quart. J. Roy. Meteor. Soc., 98, 563-589.

Kaimal, J.C., 1973: *Turbulence spectra, length scales and structure parameters in the stable surface layer.* Boundary-Layer Meteorol., 4, 289-309.

Kaimal, J.C., Wyngaard, J.C., Haugen, P.A., Coté, O.R., Izumi, Y., Caughey, S.J. and Readings, C.J., 1976: *Turbulent structure in the convective boundary layer.* J. Atmos. Sci., 33, 2152-2169.

Lamb, R.G. 1978: *A numerical simulation of dispersion from an elevated point source in the convective planetary boundary layer.* Atmos. Environ. 12, 1297-1304.

Lamb, R.G., 1982: *Diffusion in the convective boundary layer*, in: Atmospheric turbulence and air pollution modelling, F.T.M. Nieuwstadt and H. van Dop, Eds. D. Reidel Publishing Company, Dodrecht, Holland, 159-229.

Lewellen, W.S. and Teske, M., 1975: *Turbulence modeling and its application to atmospheric diffusions.* Part I: *Recent program development, verification and application;* Part II: *Critical review of the use of invariant modeling.* EPA-600/4-75-16 a,b. Part I, 79 pp; Part II, 50 pp.

Mellor, G., 1973: *Analytic prediction of the properties of stratified planetary surface layers.* J. Atmos. Sci, 30, 1061-1069.

Nieuwstadt, F.T.M. and van Ulden, A.P., 1977: *Vertical dispersion of passive material from a continuous point source in the atmospheric surface layer.* Royal Netherlands Meteorological Institute, De Bilt.

Nieuwstadt, F.T.M., 1980: *Application of mixed-layer similarity to the observed dispersion from a ground level source.* J. Appl. Meteor., 19, 157-162.

Pasquille, F., 1974: *Atmospheric diffusion.* 2nd Ed. John Wiley and Sons, New York.

Richtmyer, R.D. and Morton, K.W., 1967: *Difference Methods for initial-value problems.* Interscience 405 pp.

Saab, A.E., 1979: *Contribution à l'étude du transport turbulent de masse dans l'atmosphère.* E.D.F. Bulletin de la Direction des Etudes et Recherches. Série A, Nucléaire, Hydraulique, Thermique, n^{o} 4. 211 pp.

Smedman-Högström, A-S. and Högström, U., 1975: *Spectral gap in surface layer measurements.* J. Atmos. Sci., 32, 340-350.

Smith, F.B., 1965: *The role of wind shear in horizontal diffusion of ambient particles.* Quart. J. R. Met. Soc., 91, 318-329.

Willis, G.E. and Deardorff, J.W., 1978: *A Laboratory study of dispersion from an elevated source within a modeled convective planetary boundary layer.* Atmos. Environ., 12, 1305-1311.

Willis, G.E. and Deardorff, J.W., 1981: *A Laboratory study of dispersion from a source in the middle of the convective mixed layer.* Atmos. Environ., 15, 109-117.

Yamada, T. and Mellor, G., 1975: *A simulation of the Wangara atmospheric boundary layer data.* J. Atmos. Sci., 32, 2309-2329.

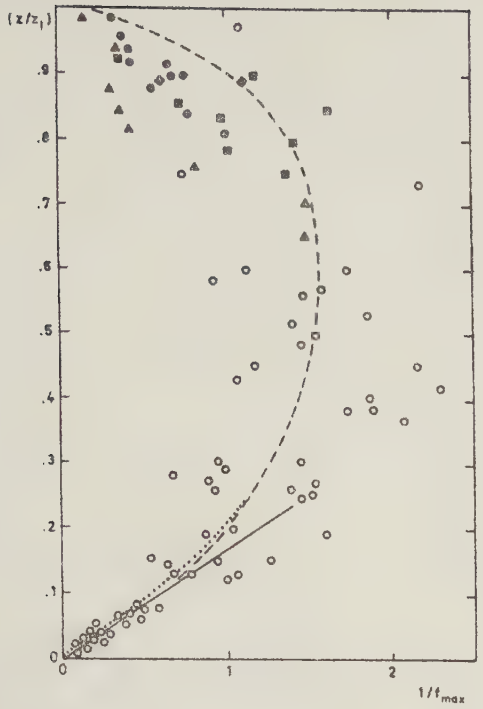

Fig 1. The variation of the normalized peak wavelength for the vertical velocity component with z/z_i. The full line represents the free-convection prediction, the dashed line represents relationship (37) and the dotted line represents relationship (38).

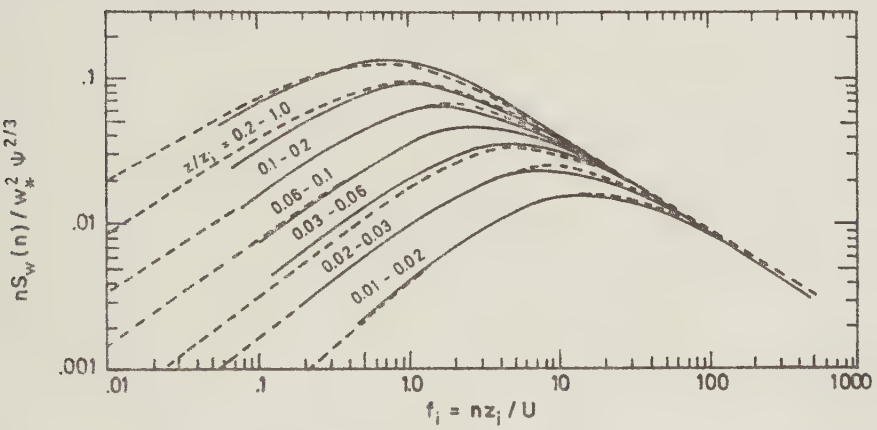

Fig 2. Universal curves for the vertical velocity spectra expressed in mixing layer similarity coordinates. The dashed lines represent the relationship (35) together with the relationships (36) and (39).

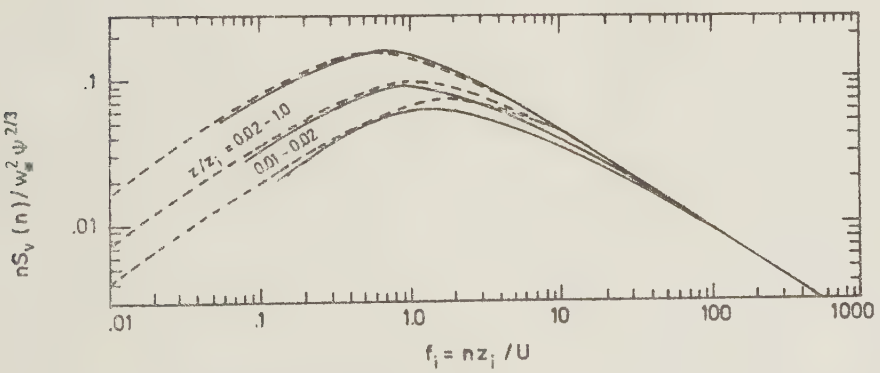

Fig 3. Universal curves for the cross-wind velocity spectra expressed in mixing layer similarity coordinates. The dashed lines represent the relationship (35) together with the relationships for b and f_{max} (cf. text).

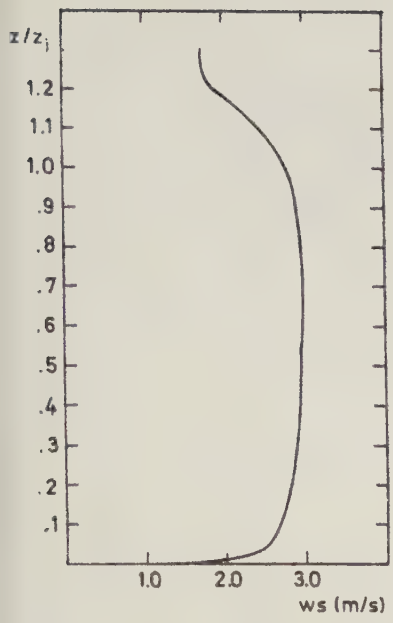

Fig 4. Computed mean wind-speed as a function of the normalized height z/z_i used in the simulations of the convective boundary layer (cf. text).

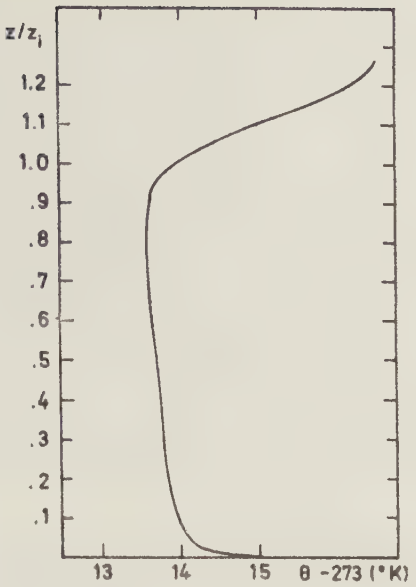

Fig 5. As Fig 4 except for mean potential temperature.

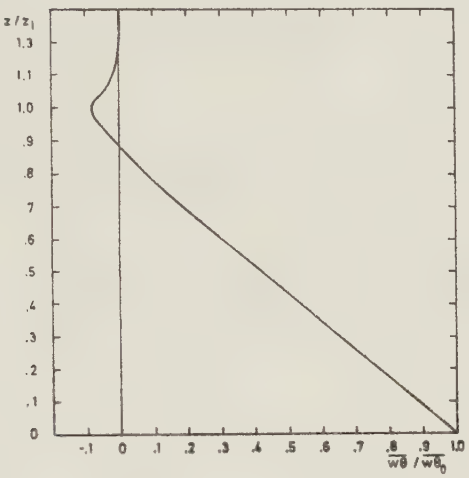

Fig 6. As Fig 4 except for normalized heat flux.

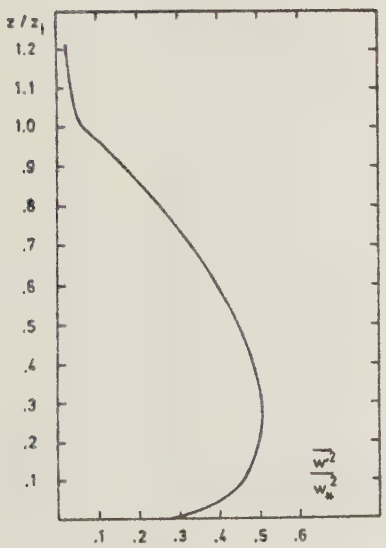

Fig 7. As Fig 4 except for normalized vertical velocity variance.

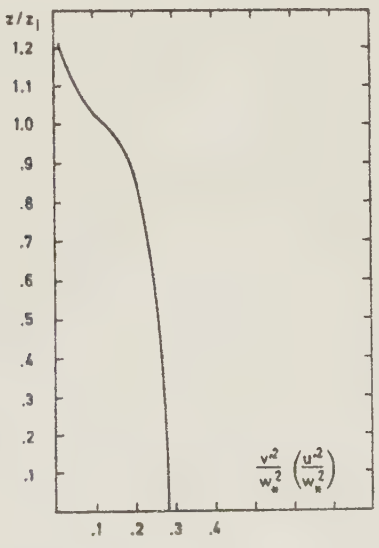

Fig 8. As Fig 4 except for normalized horizontal velocity variance.

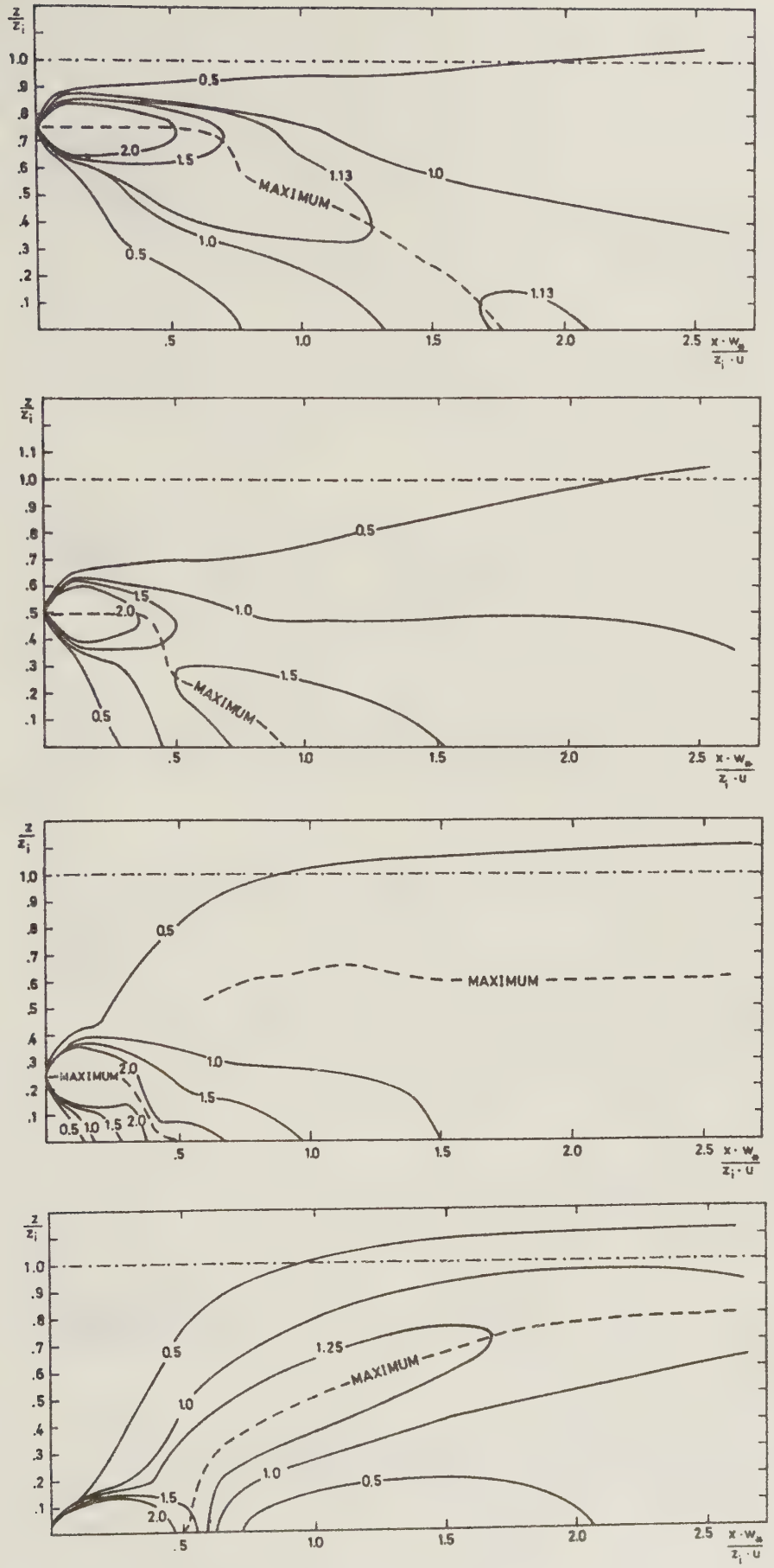

Fig 9. Calculated non-dimensional cross-wind integrated concentration $C_y\ z_i\ U/Q_0$ for point sources of heights z_s = 0.025 z_i, 0.25 z_i, 0.5 z_i and 0.75 z_i.

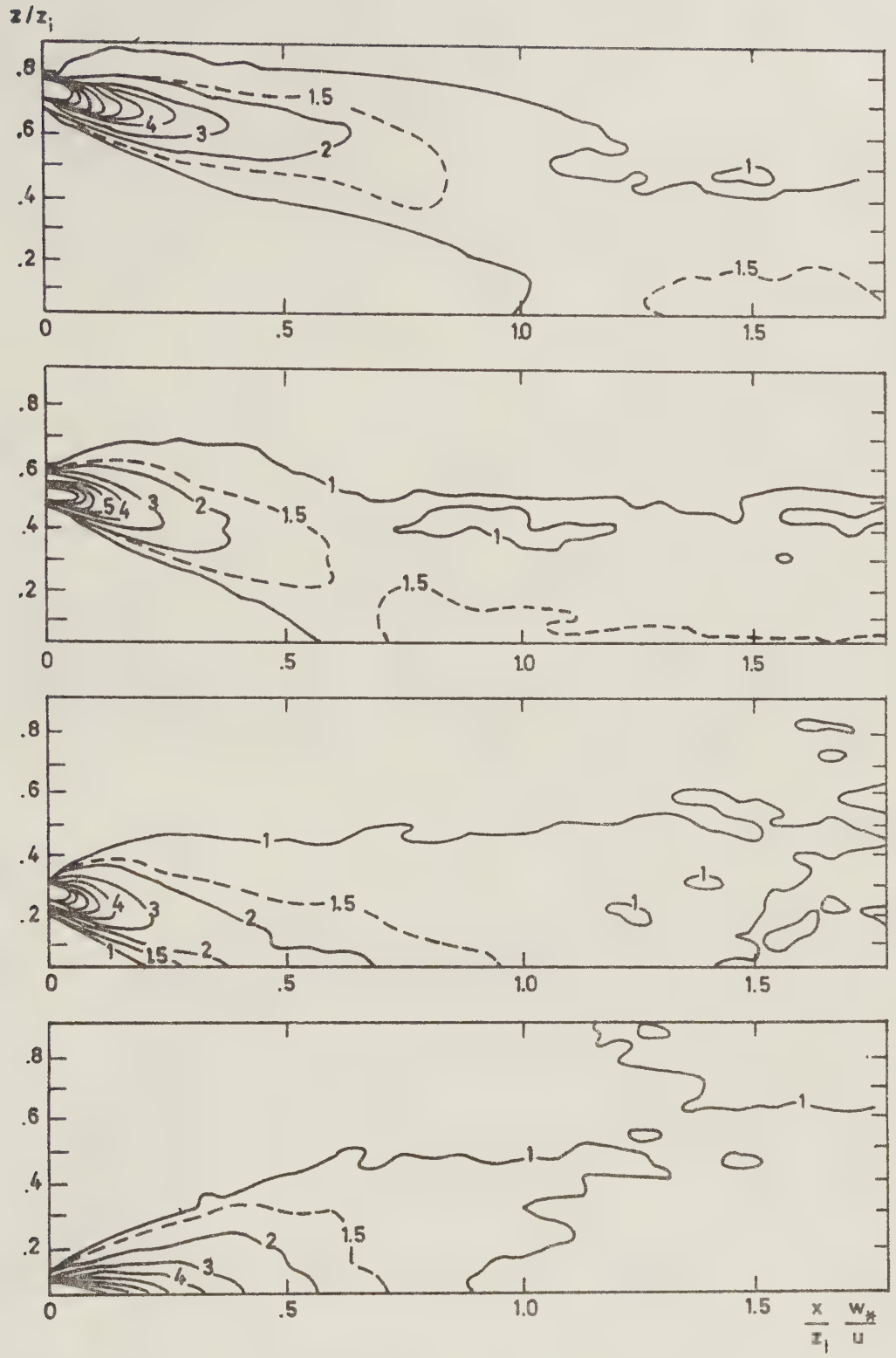

Fig 10. As Fig 9 but according to a Lagrangian model (Lamb 1982).

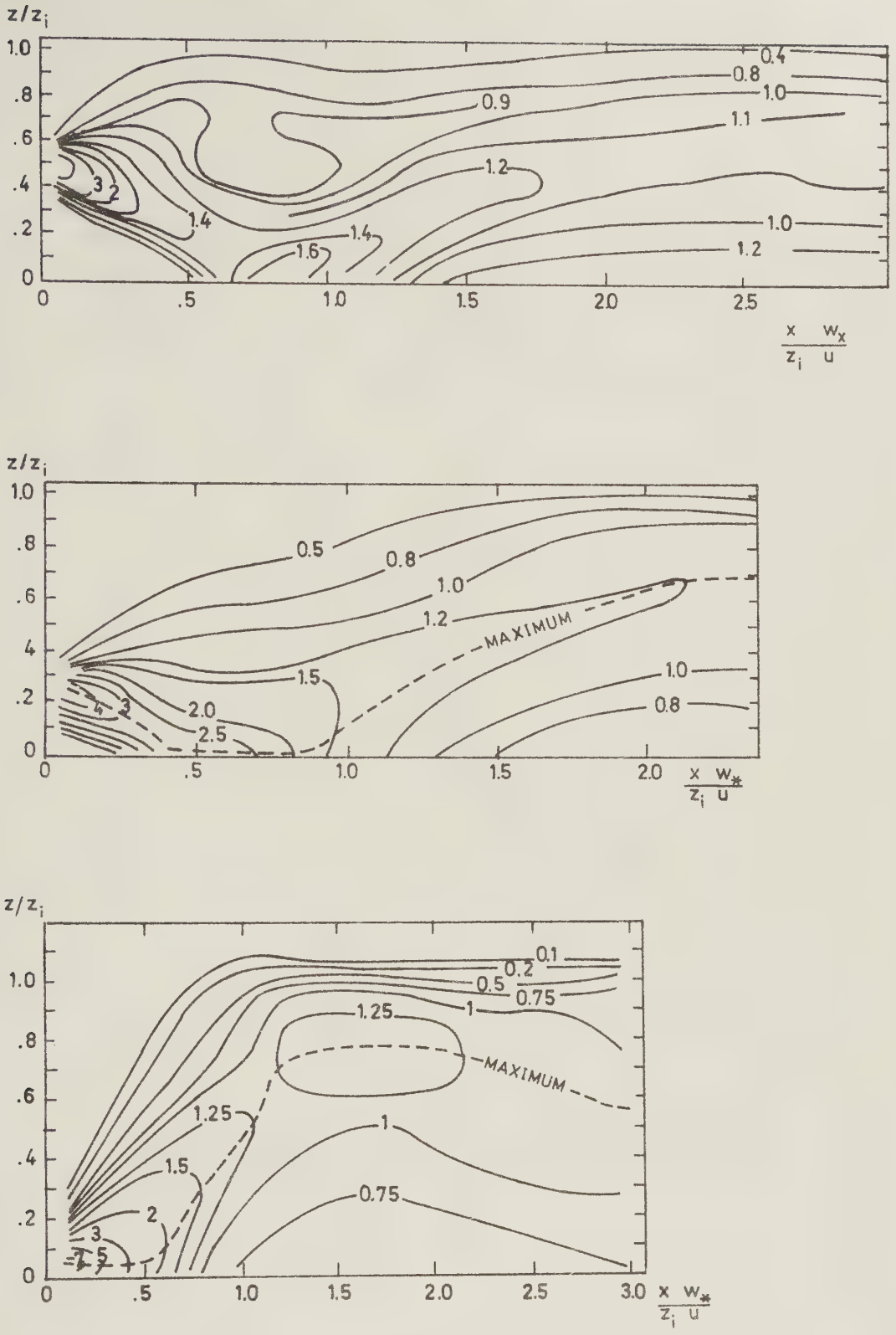

Fig 11. Experimentally determined non-dimensional cross-wind integrated concentration for point sources of heights z_s = 0.067 z_i, 0.25 z_i and 0.5 z_i (Deardorff and Willis, 1975, Willis and Deardorff, 1978 and 1981).

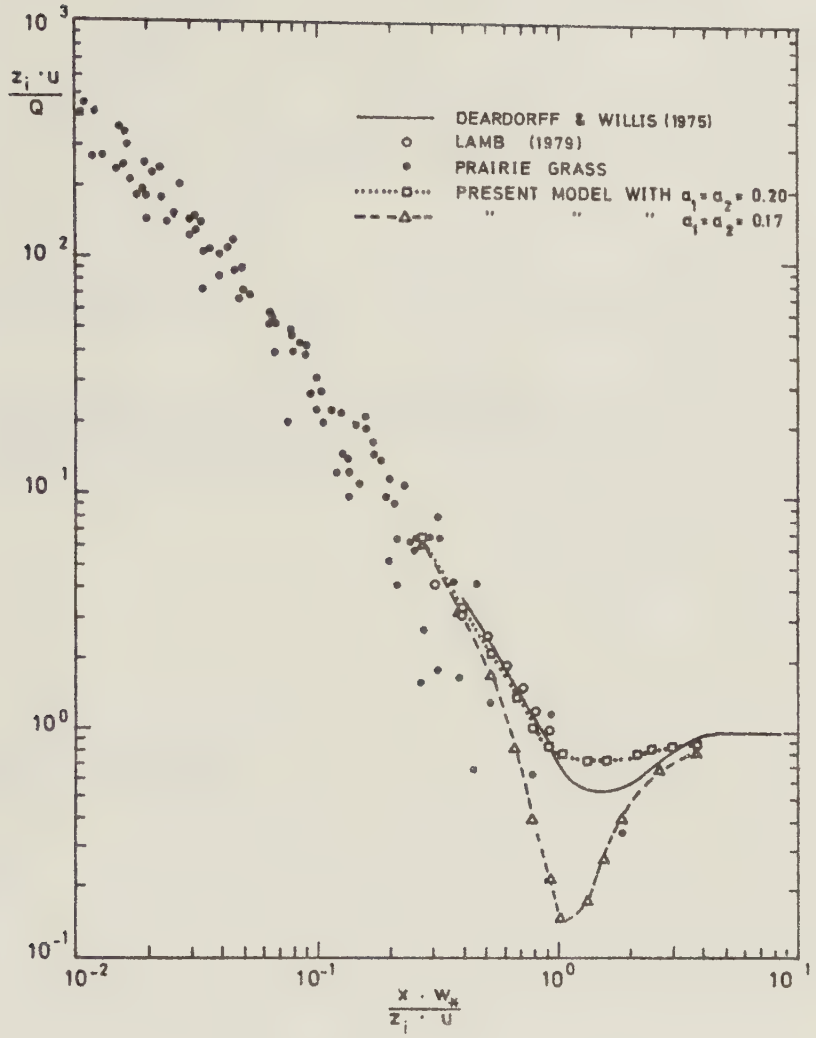

Fig 12. The dimensionless cross-wind integrated concentration at ground level as a function of the mixing layer scaling variable $x\ w_*/z_i u$.

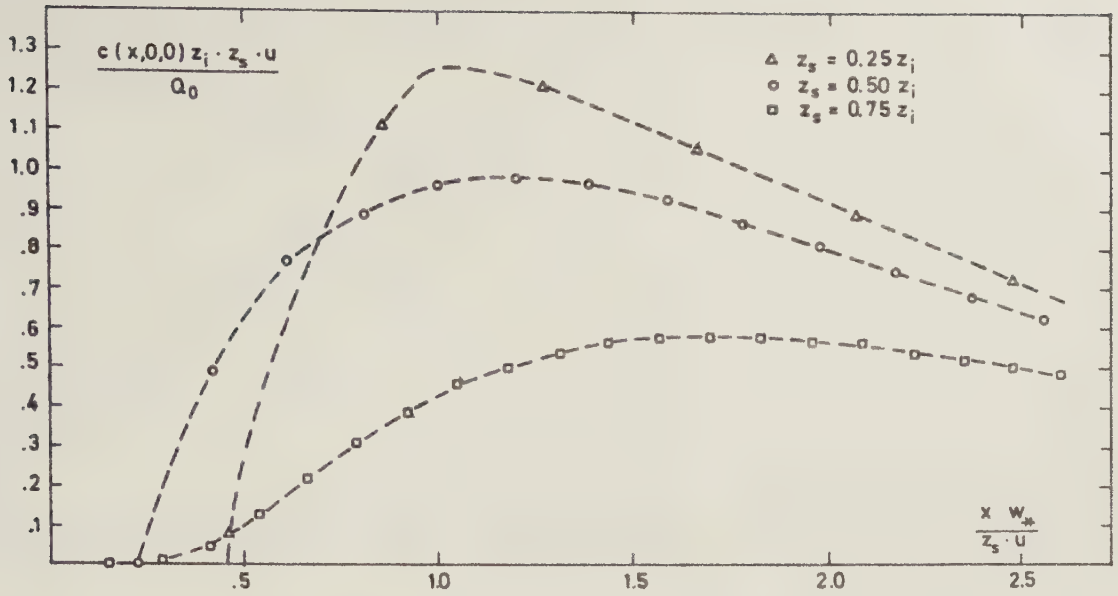

Fig 13. Calculated profiles of non-dimensional ground level concentration $C(x,0,0)\cdot z_i\cdot z_s u/Q_0$ along the plume centerline for sources of heights z_s = 0.25 z_i, 0.5 z_i and 0.75 z_i.

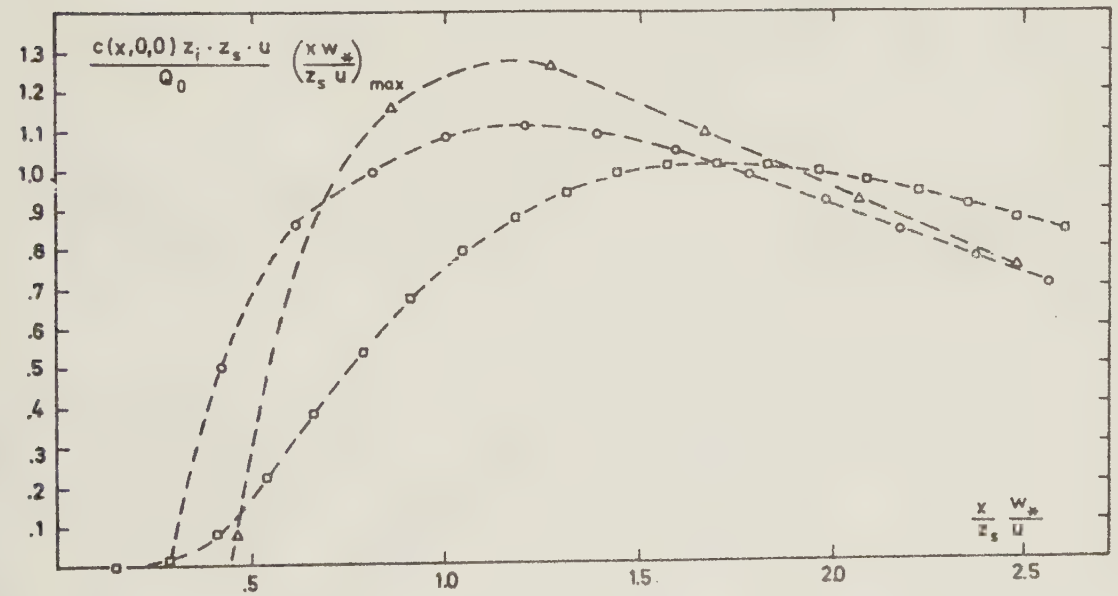

Fig 14. Calculated profiles of non-dimensional ground level concentration $C(x,0,0)\cdot z_i\cdot z_s u/Q_0\ (x\ w_*/z_s u)_{max}$ along the plume centerline for sources of heights z_s = 0.25 z_i, 0.5 z_i and 0,75 z_i.

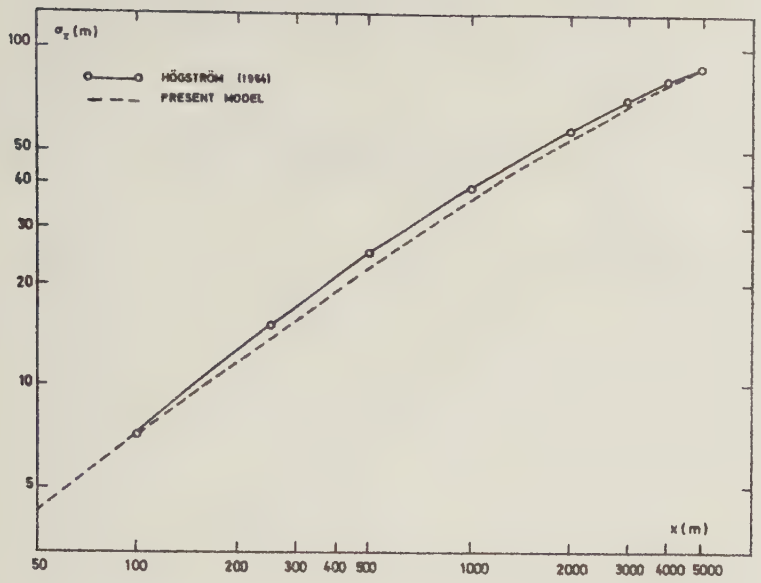

Fig 15. Comparison of the vertical standard deviation predicted by our model with the corresponding field measured (Högström, 1964) at neutral conditions for a source at 87 m height.

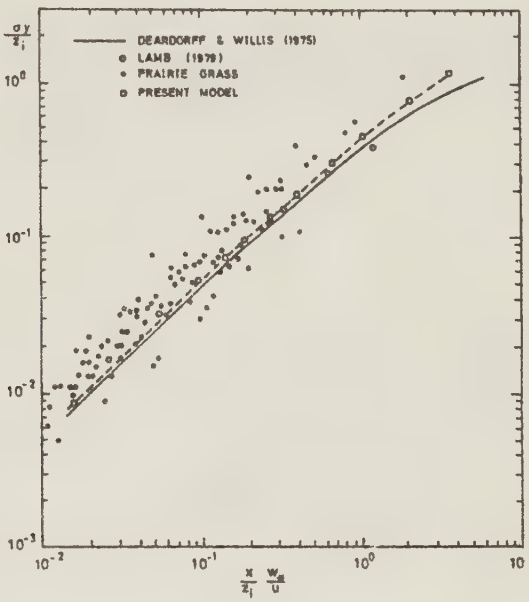

Fig 16. The dimensionless lateral standard deviation as a function of the mixing layer scaling variable $x\ w_*/z_i u$ at a release height of $0.025\ z_i$.

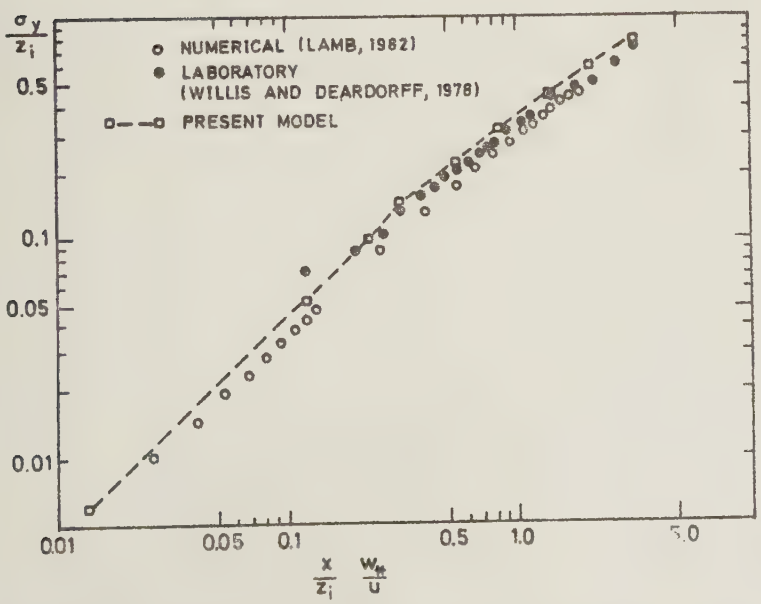

Fig 17. Comparison of the cross-wind standard deviation as a function of the mixing layer scaling variable $x\ w_*/z_i u$ at a release height of $0.25\ z_i$.

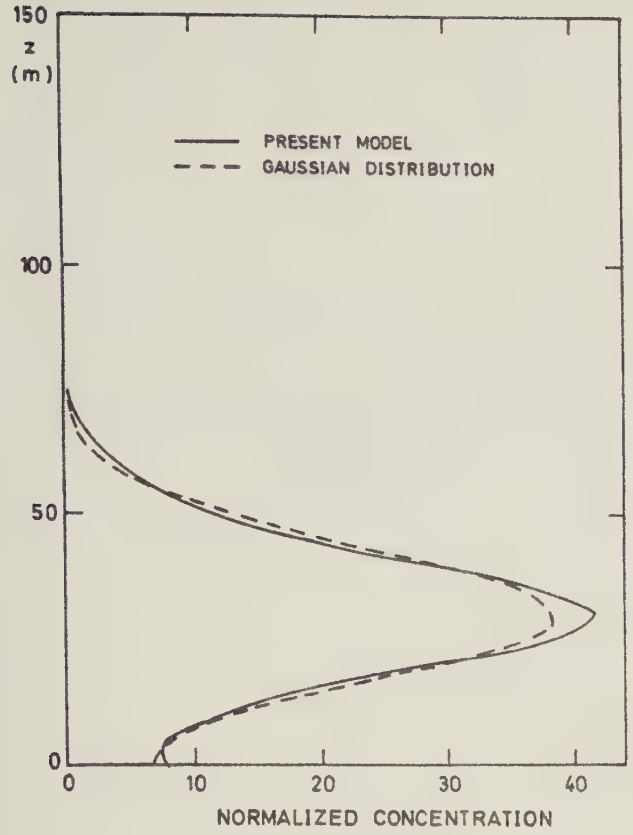

Fig 18. Comparison of the cross-wind integrated concentration determined from the present model 700 m downstream the source in a stable boundary layer with the concentration determined from a Gaussian assumption.

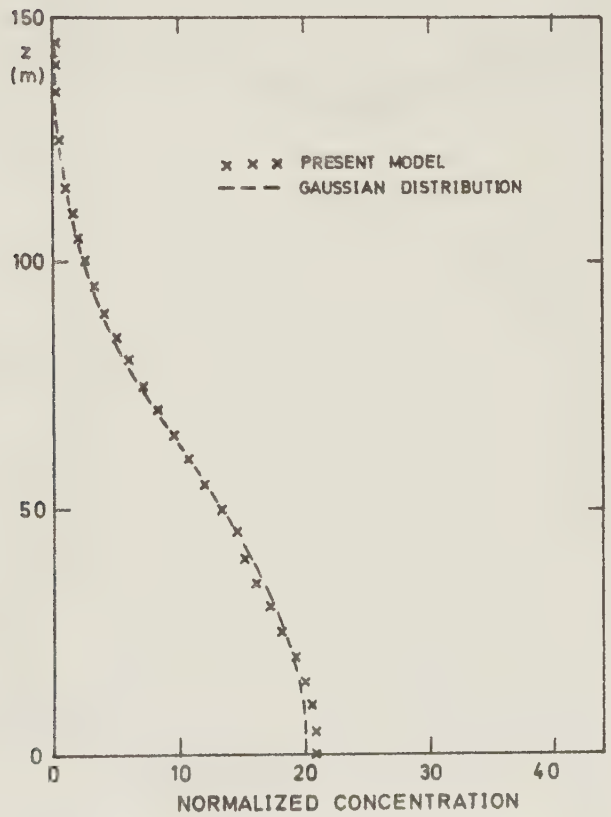

Fig 19. As Fig 18 except for 1500 m downstream the source.

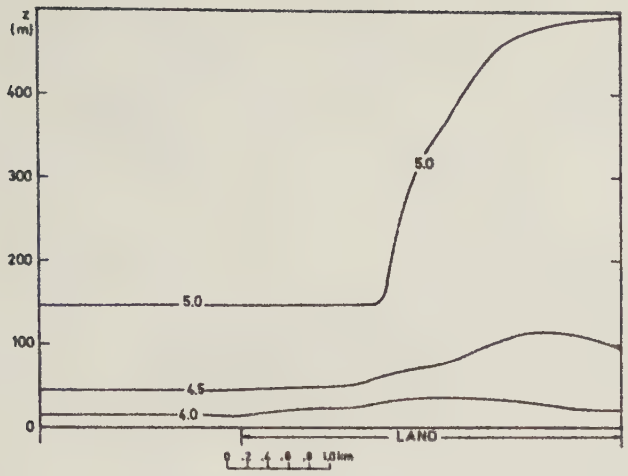

Fig 20. Space variation of the simulated wind-speed (m/s) used in the simulation of dispersion in a case with horizontally heterogeneous conditions.

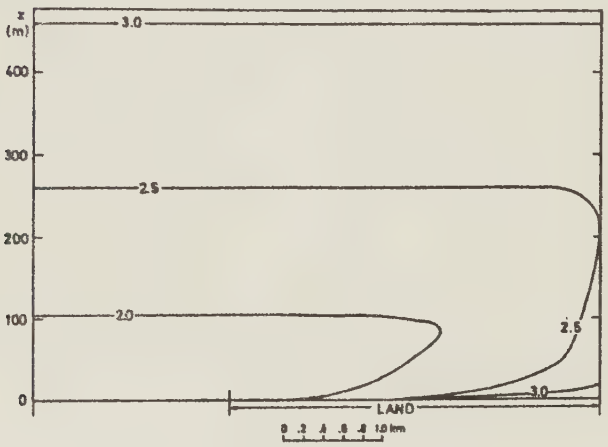

Fig 21. As Fig 20 except for the simulated potential temperature (^{o}C).

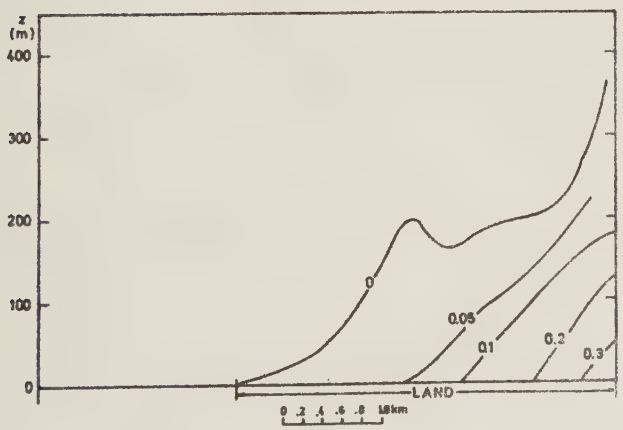

Fig 22. As Fig 20 except for the simulated kinematic heat flux ($m \cdot K\ sec^{-1}$).

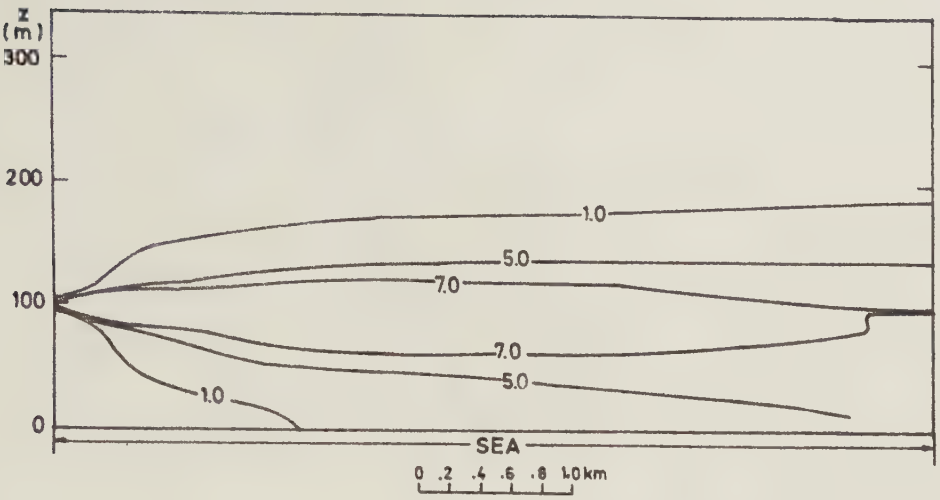

Fig 23a. The simulated cross-wind integrated concentration field over the sea in a stable boundary layer.

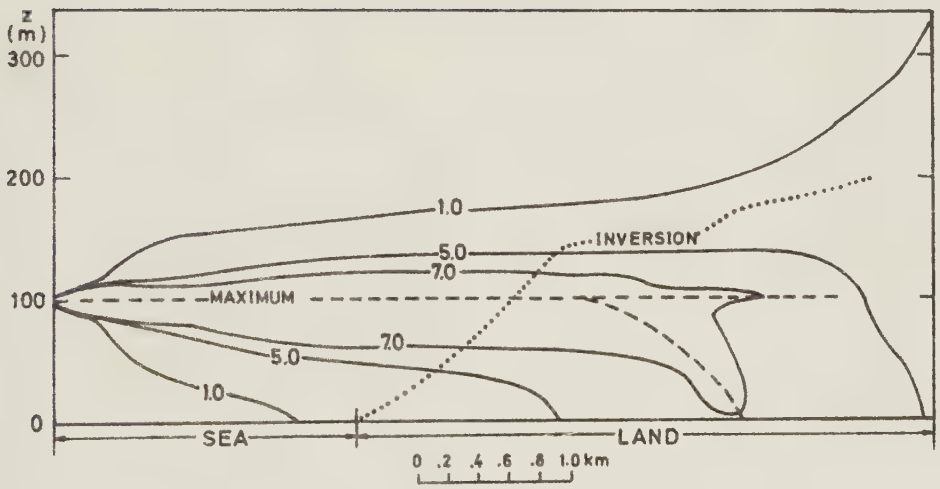

Fig 23b. As Fig 23a except with an island situated 2 km downstream the source.

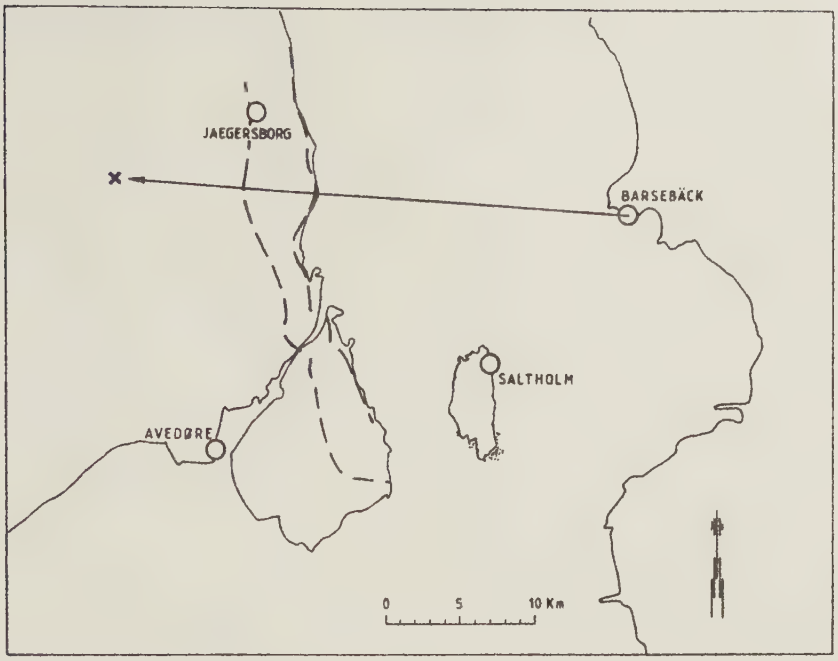

Fig 24. The experimental site. The sampling units were situated along the dashed lines. The rings show the meteorological measurement sites used in the calculations. The x-axis used in the dispersion calculations is also shown.

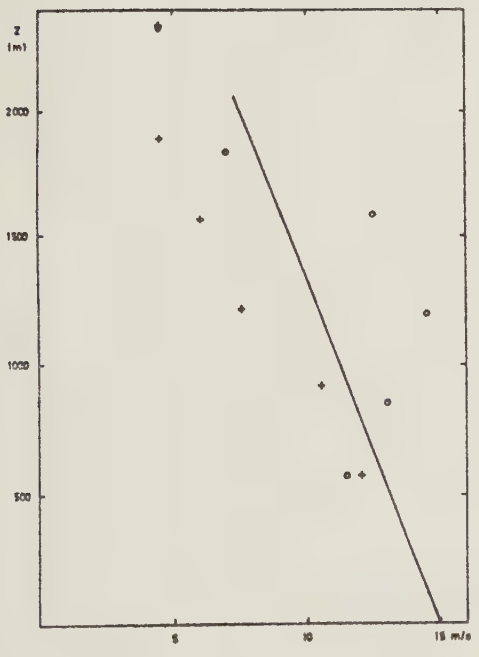

Fig 25. The full line represents the geostrophic wind-speed used in the simulations as a function of height. Crosses and rings represent measured wind-speeds on June 23, 0600 EMT and 1800 EMT respectively at Jaegersborg.

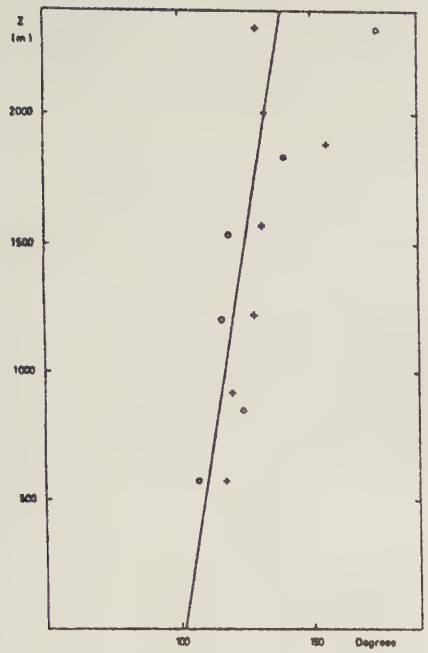

Fig 26. The full line represents the geostrophic wind direction used in the simulations as a function of height. Crosses and rings represent measured wind directions on June 23, 0600 EMT and 1800 EMT respectively at Jaegersborg.

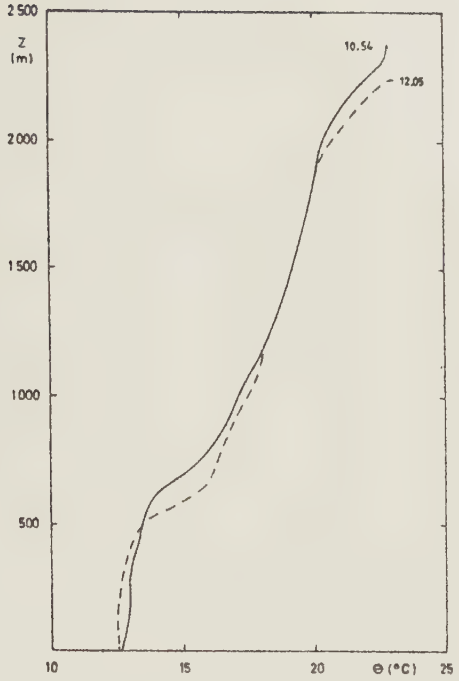

Fig 27. Measured temperature profiles at Jaegersborg June 23, 1982. The full line represents the temperature profile at 10.54 EMT and the dashed line represents the temperature profile at 12.05 EMT.

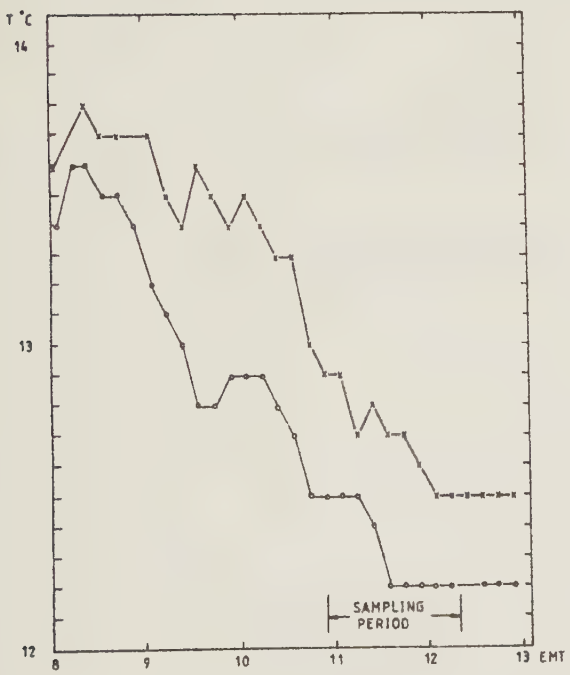

Fig 28. Time variation of the observed temperature at the 2 m level on the island of Saltholm (crosses) and at Avedøre (rings).

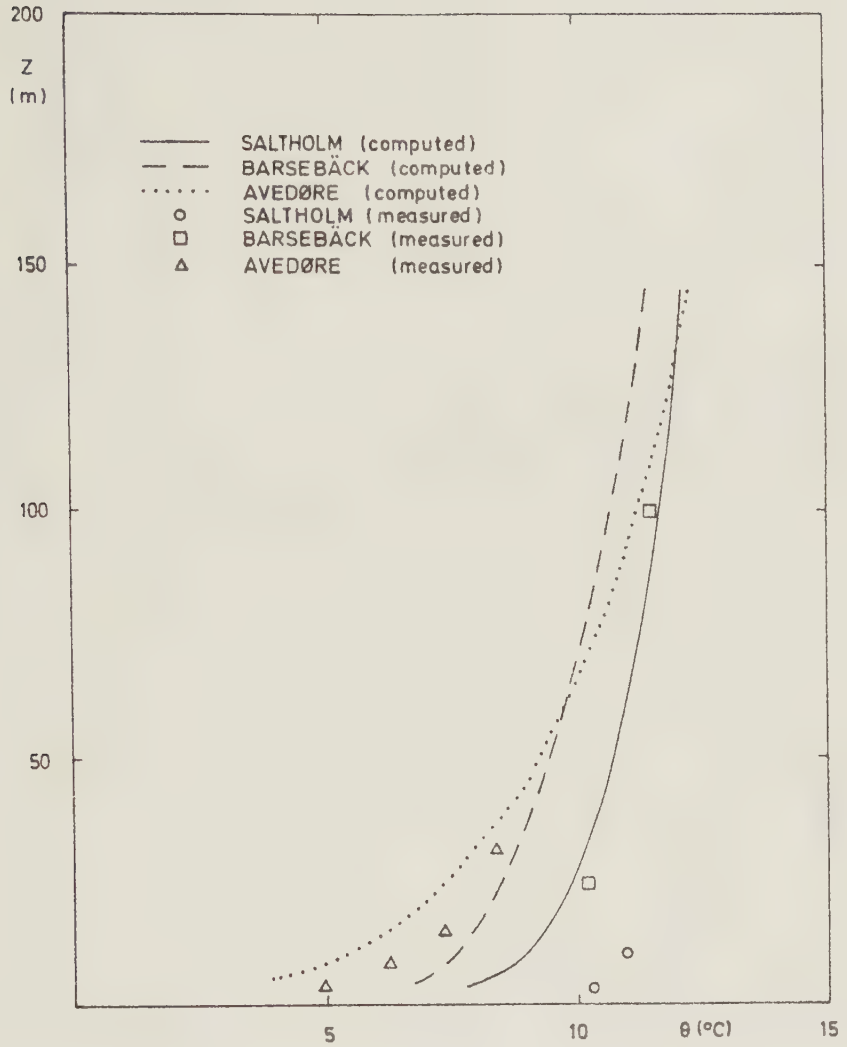

Fig 29. Observed and computed wind-speed profiles at Barsebäck, Saltholm and Avedøre.

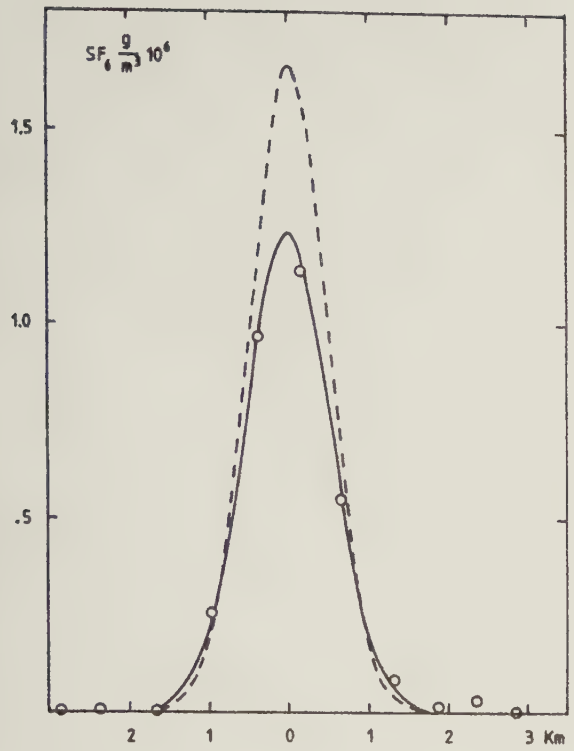

Fig 30. Observed (rings) and computed tracer concentration along the coast-line; the distance from the release point is 21 km. The full line and the dashed line represent the computed concentrations using the temperature profiles measured at 10.54 EMT and 12.05 EMT, respectively.

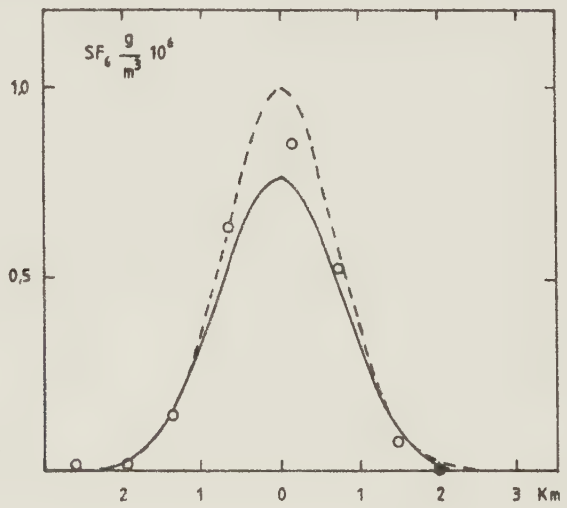

Fig 31. As Fig 30 except along the inland semi-circle; the distance from the release point is 24.5 km.

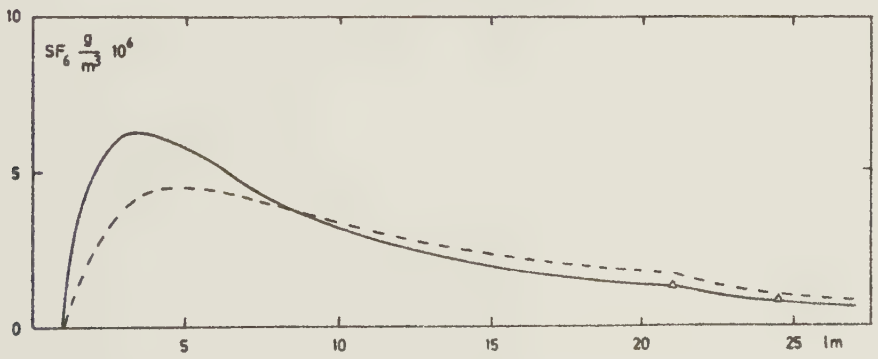

Fig 32. Observed (triangels) and computed maximum ground level concentration, C(x,0,0), as a function of distance from the release point. The full line and the dashed line are coded as in Fig 30.

Distributed by
Department of Meteorology
Uppsala University
Uppsala, SWEDEN

ISBN 91-506-0386-8